NTNU

Norwegian University of
Science and Technology

Power electronic converters for remotely operated vehicles

Håvard Edvardsen

Master of Science in Electric Power Engineering
Submission date: June 2018
Supervisor: Dimosthenis Peftitsis, IEL

Norwegian University of Science and Technology
Department of Electric Power Engineering

Abstract

Remotely operated vehicle (ROV) is considered a key component for the subsea industry. Not only for the oil and gas industry, but also for inspection of underwater installations, subsea installations of HVDC cables, object location and recovery, diver observation and assistance and so on. The ROV will play an even more important role in subsea development in the future, as the depths of interest are getting deeper.

Most commercialized ROVs today, utilizes hydraulic systems for the propulsion and tooling equipment on board. However, the industry is starting to shift focus over to fully electric ROVs and the possible advantages it presents. Lower maintenance cost, higher reliability and efficiency, and thinner and cheaper umbilical are the main driver for this shift. As the industry is moving towards operation in deeper waters than today, the shift to fully electrifying the ROVs is even more crucial.

This thesis investigates the converter suited as the main converter for the ROV. The main converter is supplied with medium voltage from the umbilical and it distributes a low voltage to the equipment on board the ROV. The converter must be dimensioned to handle the entire load of the ROV. Since the hydraulic power unit, which is the biggest load, is removed from the ROV when fully electrifying the ROV, the power rating for the ROVs does not need to be as high as the hydraulic ROVs. After discussion with the industry, a 100 kW power rating has been used for this thesis.

In the literature study leading up to this thesis, a new electrical system was proposed for the fully electric ROV. The study points to several benefits for the electric ROV and suggests that the ROV is supplied with a MVDC at 3 – 15 kV through the umbilical and a LVDC at 0.4 – 0.7 kV as the power supply on the ROV. The study also suggest that a galvanic isolation is needed to ensure safe operations and obtain higher reliability. This means that the main converter should be designed as an isolated DC/DC converter.

Five different converter topologies have been presented and discussed. They all have their advantages and disadvantages. One of the most important criteria for ROV application is weight and volume. Converter efficiency is second priority. This means that the converters should be optimized to avoid high capacitances and inductances.

Two of the presented topologies are further designed, simulated and evaluated for the ROV application; the dual active bridge and the modularized dual active bridge. Since the voltage or switching frequency is not clear at this point, several voltage and frequencies ranges has been tested in order to optimize the design.

The result from calculation and simulation shows that by choosing the modularized dual active bridge the volume can be decreased by more than 57 % compared to the dual active bridge. The reason for decreased volume is that the modularized dual active bridge can operate with a much higher switching frequency due to low voltage switches. By increasing the frequency, the passive components such as capacitors, inductors and transformers can be significantly reduced. However, this thesis has not been able to identify the complete volume of each converter. This means that the total volume of the converters in this thesis may be higher. Still, the conclusion from this thesis gives an indication for further research and development for the ROV application.

Table of content

Table of figures

Table of tables

Abbreviations

Acronym	Definition
HPU	Hydraulic power unit
SPS	Single phase-shift
DPS	Dual phase-shift
TPS	Triple phase-shift
ISOP	Input-series-output-parallel
IPOP	Input-parallel-output-parallel
MV/MP	Medium voltage / medium power
SAB	Single active bridge
DHB	Dual active half-bridge
3ph-DAB	3-phase dual active bridge
DAB	Dual active bridge
MDAB	Modularized dual active bridge

1 Introduction

This report is the master thesis for the fifth year at the Norwegian University of Science and Technology. The master thesis represents 30 ECTS-credits and is written during the spring semester of 2018. The thesis focuses on power electronics, and more specific, power electronic converters for remotely operated vehicles.

Remotely operated vehicle is considered a key component for various subsea operations. This refers not only to the oil and gas sector, but also for other subsea operations such as inspection of underwater installations, object location and recovery, diver observation and assistance, installations of HVDC cables, and so on. In the future, the ROV will play an even more important role in subsea development, as the depths of interest are getting deeper.

The ROVs today, uses hydraulic power for the propulsion and tools on board. A trend to modernize the ROVs by electrifying them is observed. The possible advantages it presents are among higher reliability and efficiency, lower maintenance cost and thinner and cheaper umbilical. The shift to fully electrifying the ROVs is even more crucial as the industry is moving towards operation in deeper waters than today.

The methods used in most of the commercialized work class ROVs features a hybrid solution of both electric power and hydraulic power. Some state-of-the-art commercialized ROVs offer the possibility to connect electrical tools in addition to the standardized hydraulic tools. This solution still requires the heavy and bulky hydraulic power unit (HPU) and represents a higher environmental impact if the HPU is damaged and hydraulic oil leaks out into the ocean. The industry is now trying to fully electrify the ROV by removing the HPU and its poor efficiency and poor environmental impact.

This thesis investigates different converter topologies that may be suitable for the ROV application. There are several design requirements that need to be fulfilled to operate properly on the ROV, such as high reliability, low maintenance and low weight and volume. The converters will be simulated and evaluated to determine their performance. The thesis will conclude with one or two converters that are suitable for the work class ROV.

2 Brief introduction to the work class ROV electrical system

The ROVs are divided into three different classes; observation class, work class and trenching and burial class. The commercially available work class ROV usually operates in depths up to 3000 - 4000 meters of seawater but it can also be designed to operate at deeper depths up to 7000 meters. [1]

The ROVs are fitted with different tools and equipment depending on their mission. The work class ROV can be fitted with a collection basket to collect samples from the sea bed and other objects in the sea, and it can have two robotic arms, called manipulators, to perform tasks below the surface. Figure 2.1 shows the Perry XLX EVO work class ROV with its tools and equipment.

Figure 2.1: The tools and equipment of the PERRY XLX EVO [2]

The electrical system on the existing commercialized work class ROV commonly uses a combination of both AC and DC. The hydraulic power unit (HPU) is usually supplied with HVAC up to 3.3 kV, while the electronics and thrusters (if not hydraulic) requires a low DC voltage of typically 12 – 600 V. [1] [3] [4]

Table 2.1: Voltage rating of different components on the work class ROV [1] [3] [4]

Equipment	Voltage [V]	AC or DC
HPU	2850 – 3300	AC
Thrusters	45 – 600	AC or DC
Manipulators, tools	24 – 380	DC
Cameras, sensors, lights	12 – 24	DC

The frequency of the high voltage from the vessel to the ROV is commonly higher than 50/60 Hz. Some manufacturers operate with a frequency of 400, 480 or 800 Hz [3]. As shown in figure 2.2, increasing the frequency up to 1 kHz has negligible effect on the AC-resistance [5]. The advantage of choosing a higher frequency is to enable smaller and lighter transformer and other passive components. This saves weight and space where the transformer and components are placed.

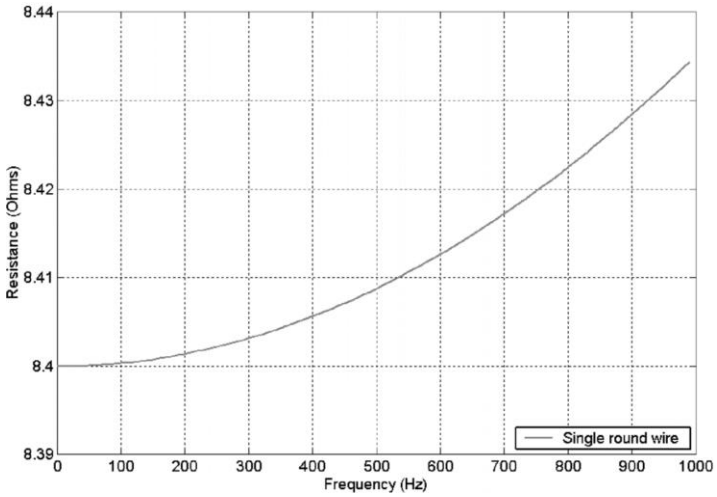

Figure 2.2: Transmission frequency vs resistance [5]

The power consumption of a work class ROV is about 100 kW and higher. The main consumer of power is the hydraulic power unit. It can range from 75 to 200 kW depending on the size of the ROV. If the thrusters are electric, they can typically consume from 3 to 12 kW. Some ROVs are equipped with the possibility to have electrical tooling, which has a power consumption up to 135 kW.

Table 2.2: Power ratings of different components on the work class ROV [1] [6]

Equipment	Power [kW]
Entire ROV	> 100
HPU	75 – 200
1 pc. thruster	3 – 12
Manipulator/Tooling	< 135
Camera, sensor, light	3 – 6

3 Theory

In the literature study leading up to this thesis, an electrical system for a fully electric work class was proposed. Figure 3.1 shows the proposed system. Both an AC and a DC system is proposed but in this thesis a DC voltage system is used for the transmission voltage through the umbilical and for the power network on the ROV.

The vessel supplies a 3-phase low voltage of 400 – 690 VAC to a transformer that steppes the voltage up to a medium voltage for transmission. The medium voltage level is in the range of 3 – 15 kV. The medium voltage is then fed through a rectifier which converters the 3-phase AC voltage into a DC voltage. The MVDC is fed through the umbilical and into the main converter for the ROV. The main converter supplies the DC bus on the ROV with a low voltage in the range of 300 – 1000 VDC. The different equipment for the ROV is connected to the DC bus. If AC equipment is connected, an inverter is required for the equipment. The different equipment have voltage requirements as shown in table 2.1 and figure 3.1.

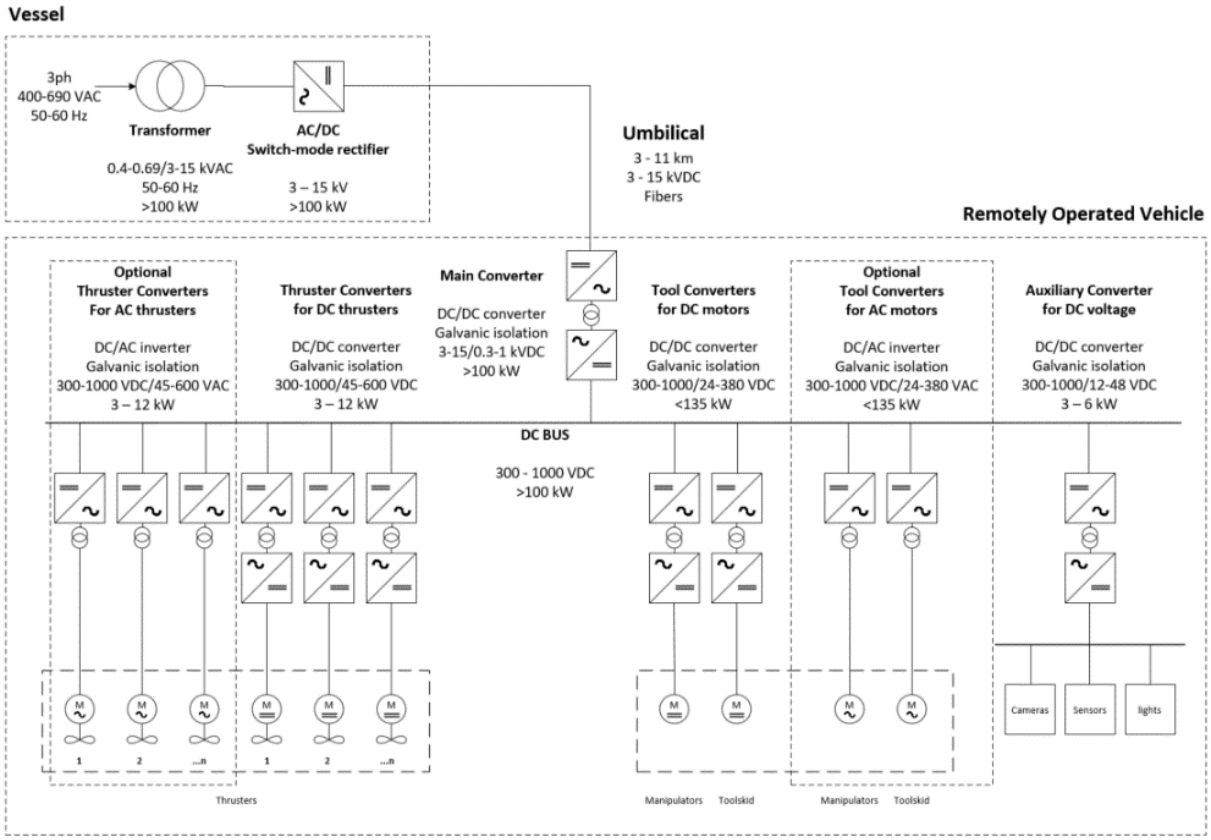

Figure 3.1: Electric system layout for the fully electric work class ROV proposed in [7]

Power consumption

The power rating of the work class ROV ranges from 100 kW up to 300 kW. As the HPU unit is removed on the fully electric ROV, the major power consumer is eliminated. The power consumption for the electric propulsion and tooling system may be lower than the consumption of the HPU. This means that the power consumption on the fully electric ROV will be lower for the same ROV as if it was hydraulic [8]. The calculation of the steady-state supply current for different voltage and power levels are shown in table 3.1.

Table 3.1: Dimensioning DC current for different voltage and power levels

	0.4 kV	**0.7 kV**	**3.0 kV**	**4.5 kV**	**6.0 kV**	**10 kV**	**15 kV**	
100 kW	250.00	142.86	33.33	22.22	16.67	10.00	6.67	[A]
200 kW	500.00	285.71	66.67	44.44	33.33	20.00	13.33	[A]
300 kW	750.00	428.57	100.00	66.67	50.00	30.00	20.00	[A]

The load profile for the ROV during operation is unknown, but from an interview with engineers in the company Oceaneering [8] some details about the power consumption during operations has become known;

- During start-up before an operation the power consumption is limited to the power loss in the system and some small loads such as electronic systems. The load is estimated to 200 W
- The load during operation is low compared to the rated power. While the ROV must be dimensioned to handle full load, the thrusters and tools rarely exceeds 20 % of rated power. This means that during operation the load is estimated to be 20 % of rated ROV power.

For this thesis, the main converter will be designed for a 100 kW work class ROV.

Voltage level

The work class ROVs on the marked today usually use a three-phase AC voltage of 3.3 kV from the vessel to the ROV. This voltage is directly connected to the HPU motor before it is connected to a transformer for the low voltage equipment. The low voltage distribution on the ROV is usually 110 V and 24 V. For ROVs with electric thrusters, it is common to have a distribution of 400 VAC as well. [1] [8]

For the fully electric ROV, a DC voltage will be used to transfer the power to the ROV. The DC voltage could be in the range of 3 – 15 kV. The main reason for limiting the voltage is the voltage rating of the switching devices. For the switching devices to handle very high voltages they must be series connected which may lead to a bigger and bulkier converter, more challenging switching processes and gate driver designs, higher complexity and lower reliability for the converter. The output voltage of the converter can be in the range of 0.3 – 1.0 kV DC.

The rated input and output voltage of the converter will be evaluated for each converter design. The maximum voltage ripple is set according to the DNV standard (DNVGL-OS-D201) and cannot exceed 10 %.

Switching devices

The switches available for power electronic converters at rated voltages above 1 kV are limited. Silicon MOSFETs are available for voltages up to 1.7 kV, but they have very high on-state resistance which leads to very high losses [9]. The realistically highest blocking voltage for silicon MOSFETs are up to 0.9 kV [10]. Silicon JFET and bipolar junction transistors (BJT) have both a maximum blocking voltage capability of around 1 kV. IGBTs combines the best features of the MOSFET and BJT, and achieves fast switching characteristics and low on-state resistance [11]. IGBTs have a maximum rated blocking voltage up to 6.5 kV [10].

During switching transients, overvoltage will appear due to the stray inductance in the switching device and the network. These voltage spikes can be calculated by using equation 3.1, but since the stray inductance of the network is unknown the voltage spikes cannot be properly calculated. A safety margin of 1/3 is therefore applied and the IGBTs will be dimensioned by 2/3 of their maximum blocking voltage.

$$V_{overvoltage} = L_{stray} \frac{di}{dt} \qquad 3.1$$

Switching frequency

The switching frequency is limited by the capability of the devices in the converter. The design of each converter is mainly deciding the possible switching device and thus switching frequency.

For the IGBT switching devices the switching frequency is limited due to the tail current at turn-off. The recommended maximum switching frequency for the IGBT devices are in the range of up 10-15 kHz for the lower medium voltages. For the 6.5 kV IGBT devices they should be reduced to a maximum of 5 kHz for the highest currents [12]. However, a lower switching frequency may be desirable to avoid high switching losses. For this study a switching frequency of 5, 10 and 15 kHz will be used for comparison for all converter topologies using IGBT devices.

For the low voltage converter designs, either Silicon (Si), Silicon Carbide (SiC) or Gallium Nitride (GaN) devices can be used. Since the converter will be modular the voltage across each device is lower. Low voltage enables the use of MOSFETs which allows for a much higher switching frequency compared to IGBTs. This leads to smaller passive components such as capacitors, inductors and transformer.

Low voltage Si MOSFETs has a maximum switching frequency capability up to 100 kHz [13]. The frequency is limited due to, among other things, the radical increase in conduction losses at higher frequency, even though the switching losses are low for Si MOSFETs. [14]

For the SiC and GaN devices a switching frequency of up to several hundreds of kilohertz, and even several tens of megahertz for GaN, is possible [14] [15]. However, the switching and conduction losses may be very high for the highest frequencies. A frequency of 50, 100 and 200 kHz is chosen for comparison for the SiC and GaN devices.

Isolation transformer for medium frequency

The isolation transformer is usually the component consuming the most volume in the converter. Due to its high-power rating the transformer will be very large and heavy. Thankfully, due to the high switching frequencies, the transformer size and weight will be drastically reduced.

It is difficult to find the exact specifications for a transformer that would fit to this master thesis, but there are some research and references for a similar transformer. In table 3.2 different prototypes and commercially available medium frequency transformer are listed. The table are sorted by switching frequency and power rating.

Table 3.2: Comparison of medium-frequency transformers [16] [17]

Manufacturer	f_{sw} [kHz]	Power [kVA]	V_{in} [kV]	V_{out} [kV]	Cooling	Power density [kW/dm^3]	Power density [kW/kg]
ABB	1.75	150	1.8	0.75	Oil	2.4	1.1
ALSTOM	5	1500	1.8	1.65	Oil	2.1	1.5
UEN	5.6	450	3.6	3.6	Liquid/Oil	-	18.8
Bombardier	8	350	1	1	Liquid	-	7
STS	8	450	1.8	1.8	Oil/Air	-	9
EPFL	10	100	0.75	0.75	Air	8.2	3.6
ABB	10	240	0.6	0.9	Air	3.6	5.7
ABB	10	350	3	3	Liquid/Air	9.5	7
ABB	15-22	100	0.54	0.54	Oil/Air	1.1	1.1
ETHZ	20	166	0.75	0.75	Forced air	8.21	-
ETHZ	20	166	1	0.4	Liquid	32.7	16.6
ETHZ	20	1000	12	1.2	Liquid	78	-

From the table it can be seen that the transformer that is cooled with oil generally have a lower power density. If both air and oil is used, the power density increases. The best power density is achieved when liquid cooling is applied. The transformers from ETH Zürich with liquid cooling has a very high-power density. These are not commercially available, but experimental transformers.

From a ROV prospective, the transformer could be either build as a high-pressure container using oil or a similar cooling medium, or be placed inside a high-pressure container with all the other power electronics. The most important thing is that the transformer coil and windings are completely filled with fluid. Any air pockets between the transformer windings may result in a catastrophic failure when pressurized. [18]

For this master thesis, designing a transformer is not the main goal. Therefore, an existing transformer will be used and scaled using the power density for the weight and volume. For the simulation of the converters, the transformer will be modeled as ideal. The following transformer will be used;

Manufacturer	f_{sw} [kHz]	Power [kVA]	V_{in} [kV]	V_{out} [kV]	Cooling	Power density [kW/dm^3]	Power density [kW/kg]
ABB	10	350	3	3	Liquid/Air	9.5	7

The ABB transformer is chosen because it has a reasonable high-power density. It has a high voltage input and output, and it is also high powered. The switching frequency is somewhat lower than what is used in this thesis, but it is still high enough to be used for this design.

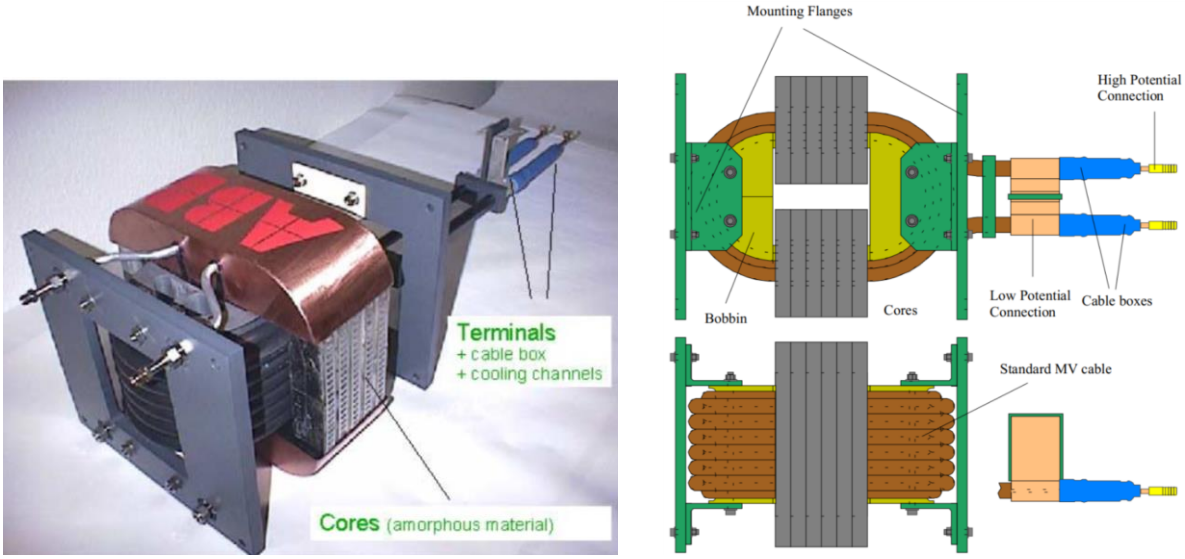

Figure 3.2: ABB medium frequency transformer [19]

Table 3.3: Specifications of ABB medium frequency transformer [19]

Condition	Symbol	Value
Rated power	P_N	350 kVA
Primary voltage	V_{PRMS}	3000 V, 50 % duty cycle, RMS
Secondary voltage	V_{SRMS}	3000 V
Turn ratio	n	1:1
Switching frequency	f_{sw}	10 kHz
Primary current	I_{PRMS}	160 (Quasi sinusoidal, RMS)
Main inductance	L_M	> 25 mH + 20% @ 10 kHz
Leakage inductance	L_σ	< 2 µH ± 10 % @ 10 kHz
Coupling capacitance	C_{PS}	≤ 3 nF
Cooling		De-ionized water
Max power loss	P_{LOSS}	< 2500 W (total)
Weight		< 50 kg
Volume		37 dm^3
Power density		9.5 kW/dm^3 - 7 kW/kg

For high frequencies above 20 kHz there is not very much data available. The transformers are usually custom made to each project and its requirements. However, some research and prototypes are found. As seen in table 3.4, the data from the research are inadequate in relation to power density. Still, the transformer from Virginia Polytechnic Institute and State University (Vtech) seem to be promising. It has an input and output voltage which correspond with the ROV application, it uses high frequency and the power density is known. The Vtech transformer data will be used for the high frequency converters in this thesis.

Table 3.4: Comparison of high-frequency transformers [20] [21] [22]

Manufacturer	f_{sw} [kHz]	Power [kW]	V_{in} [kV]	V_{out} [kV]	Cooling	Power density [kW/dm^3]	Power density [kW/kg]
ETHZ	50	25	8	0.40	Air	-	-
Chalmers	120	5.5	0.75	0.47	Air	46	-
Vtech	200	30	10	0.32	Air	17.5	-

Figure 3.3 shows the Vtech transformer prototype. The weight of the transformer is not given, but an estimated weight based on the power density and compared to the ABB medium frequency transformer gives a conservative weight of 3 kg.

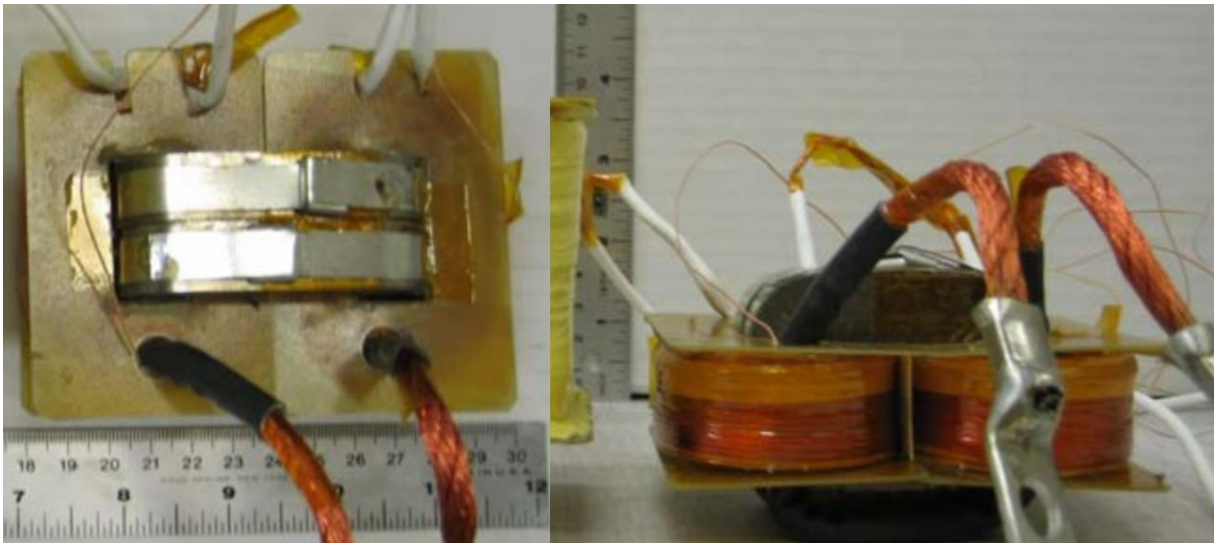

Figure 3.3: Vtech high frequency transformer (Left: top view, right: side view) [21]

Table 3.5: Specifications of Vtech high frequency transformer [21]

Condition	**Symbol**	**Value**
Rated power	P_N	30 kW
Primary voltage	V_{PRMS}	280 - 325 V
Secondary voltage	V_{SRMS}	10 000 V
Turn ratio	n	11
Switching frequency	f_{sw}	79 – 200 kHz
Max Primary current	I_{Pmax}	170 A
Average power loss	P_{loss}	603 W
Core material		Nanocrystalline (FT-3M)
Cooling		Air
Primary winding		8 turns (1518*AWG38)
Secondary winding		88 turns (136*AWG40)
Core window fill factor		0.2
Volume		1.71 dm^3
Weight (estimated)		3 kg
Power density		17.5 kW/dm^3 – 10 kW/kg

3.1 DC/DC converter topologies

For the ROV application, converters with isolation is needed to prevent electrical faults to spread throughout the electrical system on the ROV and support vessel. To achieve this the converters will have to be designed with transformers. The following chapter introduces the most commonly used DC/DC converters with isolation transformer for medium voltage and medium power (MV/MP).

The presented converter topologies are

- Dual active bridge
- Single active bridge
- Dual active half-bridge
- 3-phase dual active bridge
- Modularized dual active bridge

Dual active bridge (DAB)

The dual active bridge consists of two full-bridge converters with a high frequency transformer between. Since the rectifying stage has switches, the DAB converter is bidirectional.

The advantage compared to topologies with fewer active switches, is that the capacitor ripple problem is eliminated since the inductor current now flows through the active switches and their free-wheeling diodes instead of through passive components. In addition, the efficiency in the DAB is higher, it is more reliable and have a higher power density. Since the transmission of power is proportional to the number of switches for switches with the same current and voltage ratings, eight switches can transfer double the power as a converter using four switches [23]. Moreover, the DAB has the advantage of easy implementation of soft-switching operation and modular and symmetric structures. Only the full-bridge can generate zero output voltage and can therefore use improved modulation schemes to reduce the switching losses. [24].

One of the disadvantage with the topology is that with light load, the soft switching may be lost [25]. By using conventional phase-shift modulation the converter must be hard switched during low loads. By changing the modulation scheme to dual phase-shift control the soft-switching operation range can be expanded [23]. Other disadvantage is the total of eight switches and a relatively large magnetizing inductance of the transformer. [25]

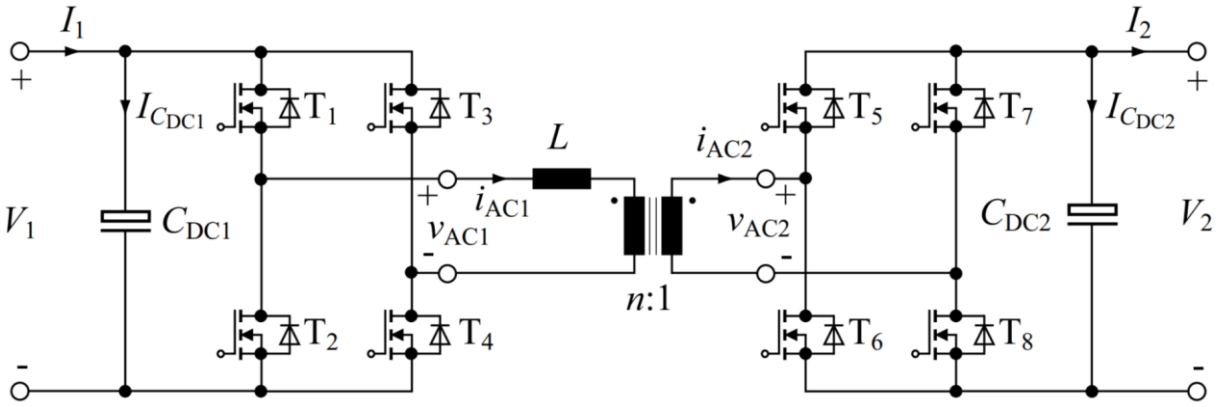

Figure 3.4: Schematic diagram of the dual active bridge [26]

The single active bridge consists of a full-bridge, a high frequency transformer and a diode bridge rectifier on the secondary side. The converter is unidirectional which only allows for power flow in one direction.

By selecting a diode rectifier in the output stage, the SAB converter can probably be reduced in volume and complexity compared to the dual active bridge. On the other hand, the output filter may be increased in volume due to higher voltage ripple.

The full-bridge inverter transforms the DC input voltage to a high frequency square wave AC voltage. The AC square voltage feed the transformer which can either transform the voltage to a higher or lower voltage, or it can have a winding relationship of 1:1. The power flow in the converter is controlled by properly controlling the switches. Two of the most common control methods are the duty cycle control and the phase-shift control. The control methods will be described further in chapter 3.2. [27] [11] [26]

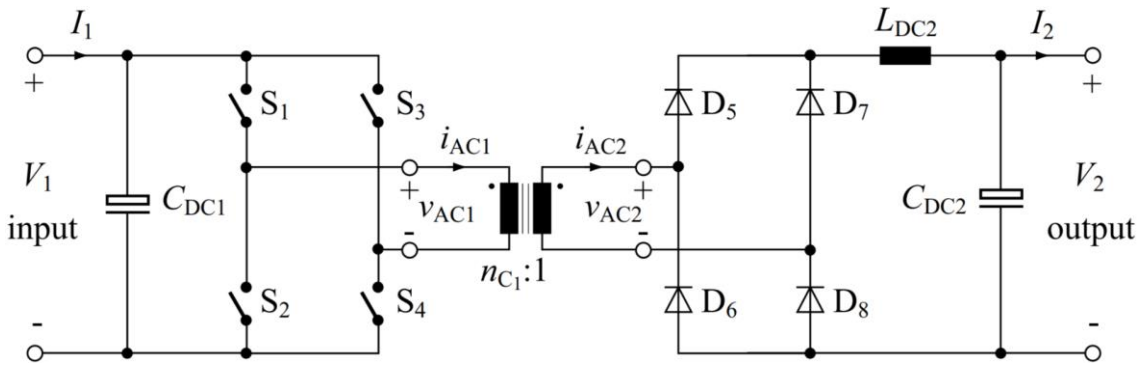

Figure 3.5: Schematic diagram of the single active bridge with output inductor [26]

Dual active half-bridge (DHB)

The dual active half-bridge is designed by connecting two half-bridges together through a high frequency transformer. The converter is a bidirectional converter which allows for power flow in both directions.

By choosing a proper inductor on the low voltage side of the converter, the current will be smoothed before the voltage is stepped up. The voltage step will then contribute to a lower primary side current stress of the transformer. The DHB can therefore be advantageous when compared to the DAB. In addition, the lower number of components could be advantageous when applying the converter for ROV application. [23] [24]

One of the main disadvantage of the converter is related to the unbalanced current stress between the low voltage switches and the ripple current flowing in the splitting capacitors. Moreover, the switching RMS current ratings are twice the RMS current of the switches used in the DAB. Another disadvantage is the size of the capacitors. [24]

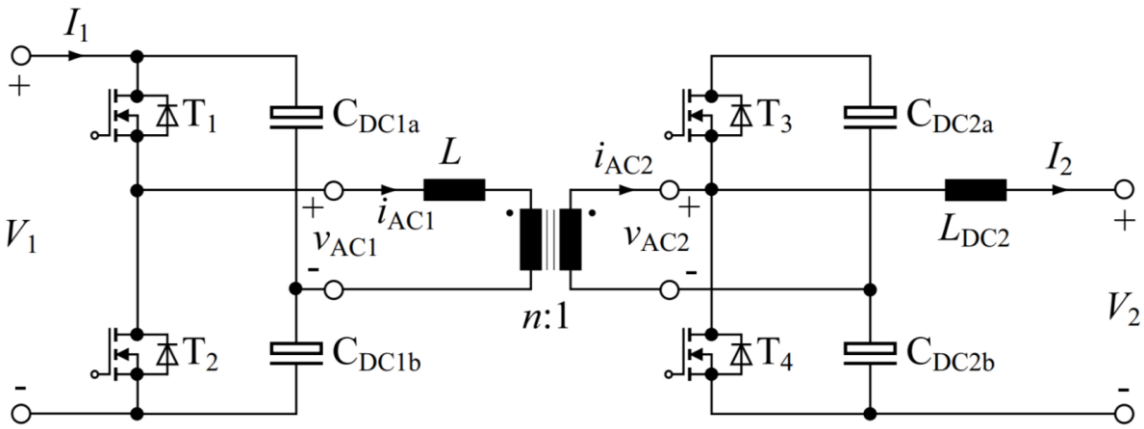

Figure 3.6: Schematic diagram of the dual active half-bridge [26]

The three-phase DAB uses three legs on each side of the high frequency transformer. It requires three inductors and three high frequency transformers, which can be made into a single three-phase transformer. The three-phase DAB can be controlled with a control scheme that is similar to the single-phase DAB. However, further performance enhancement of the modulation scheme, due to its additional phase, is not feasible for the 3ph-DAB. [26]

The 3ph-DAB shows good overall performance such as; lower switch ratings, lower transformer rating and a low magnetic energy storage capability. Compared to the single-phase DAB, the RMS capacitor currents are considerably smaller (66A vs 125A for a power level of approximate 12 kVA) according to [26].

Due to its high number of active components needed, 12 switches and accordingly 12 gate drivers, it may lead to a bulkier converter. Moreover, switching and conduction losses may be high for certain operating points due to the restrictions for the modulation scheme used. [26] [28]

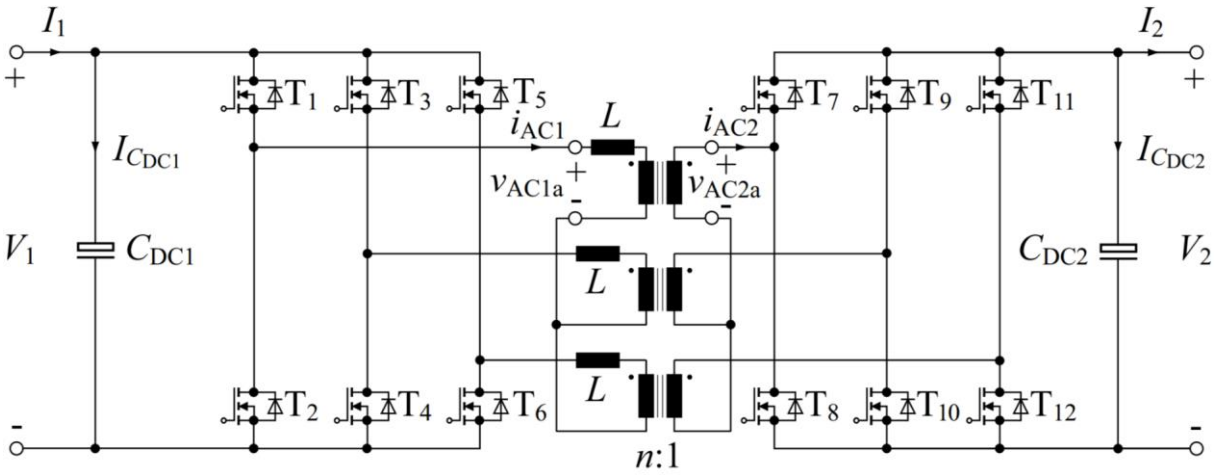

Figure 3.7: Schematic diagram of the three-phase dual active bridge [26]

To address the demand of medium voltage and high-power capability in DC-DC converters there are two methods available. The first is to either develop new semiconductor devices with higher blocking voltage capability, or series/parallel connect devices that are on the market today to reach higher blocking voltage. The second method is to develop new converter topologies with existing semiconductor devices in a modular configuration. [29]

Developing new devices is expensive and existing devices with high blocking voltage capability usually have very high switching losses when it is operating with switching frequency over 20 kHz, and therefore fail to achieve high efficiency and low power density. Modular multilevel converters enable low-voltage switching devices to handle the medium input voltage. [29]

Some of the advantages of using a modular converters are; 1) higher reliability by introducing a desired level of redundancy; 2) easier maintenance and reduction of manufacturing time and cost due to standardization of components; 3) the converter can easily be reconfigured to fit other input-output specifications; and 4) possibility of higher efficiency and lower power density for the overall system. [29]

The main disadvantages for the MDAB are; 1) complex control system due to the modular configuration; 2) low power rating for each module; and 3) The converter shown in reference [7] is not used commercially and is only in the research stage.

In [29] the proposed modules for the MDAB is a low-voltage dual active half-bridge. Each module is designed to have an input voltage of 500 VDC and an output of 400 VDC. Each module has a power capability of 1 kW and uses a switching frequency of 50 kHz. A prototype for lab testing is built and shown in figure 3.8. The complete converter design is shown in figure 3.9.

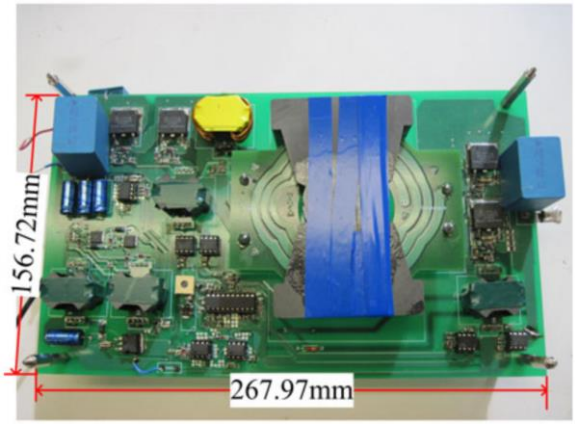

Figure 3.8: Module for experimental testing used in [29]

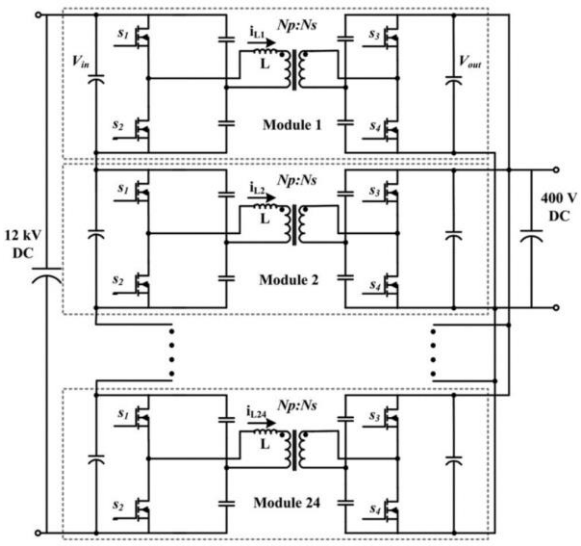

Figure 3.9: Modular converter design from [29]

3.2 Control strategy

The subchapters below explain the most common control strategies for the converters in the previous chapter. While for the SAB, variable switching frequency control have to be used due to the lack of active switches on the secondary bridge, the phase-shift modulation can be used for the other converters. Other more specialized control strategies can also be used, but for this thesis only the most common strategies are presented.

Variable switching frequency control

The variable switching frequency control is commonly used as a control method for loaded resonant converter. The resonant tanks' impedance varies with the switching frequency and thus resulting in power control. The same method can be used for the SAB topology. The voltage drop over the inductor will increase due to the increased impedance caused by a high switching frequency. This leads to a decreased inductor current, resulting in a lower output voltage. However, low switching frequencies leads to a lower impedance for the inductor, thus, higher output power. Therefore at low switching frequencies, the transformer must deliver max power and the transformer core has to be dimensioned for low frequencies. This leads to a bulky transformer. [30]

Moreover, the passive components in the converter cannot be optimized for a fixed frequency since the frequency is used as a control variable. This leads to a poor filter design. [30]

Single phase-shift control (SPS)

For the isolated DC/DC converters with active switches on both the primary and secondary side of the transformer, the SPS control is the most widely used control scheme [31]. In SPS control the switches in both sides of the transformers are switched in pairs to generate a phase-shifted square wave with a duty ratio of 50 %. Only the phase-shift angle *D* can be controlled. By controlling the phase-shift angle between the input and output voltage of the converter, the voltage across the leakage inductor of the transformer will change. Then the magnitude and power flow direction can be controlled.

SPS control has advantages such as small inertia, high dynamic and easy implementation of soft-switching control. However, since the method controls the power flow based on the transformers leakage inductance there will be a great circulating current when the voltage amplitude of the primary and secondary side of the transformer is not matched. Moreover, the RMS and peak current will increase in the converter. In addition, the converter cannot operate at zero-voltage-switching (ZVS) in the entire power range. Therefore, the power losses in the converter will be higher and hence the efficiency is reduced. [23]

Extended phase-shift control (EPS)

The EPS control is an improved method of the SPS control. The cross connected switches in one bridge are switched in pairs, while the switches in the other bridge are switched with an inner phase-shift

angle. The outer phase-shift angle, D_1, is used to control the power flow magnitude and direction, while the inner phase-shift angle, D_2, is used to decreasing the circulating power and expanding the soft-switching range.

The output voltage of the primary bridge of the isolated DC/DC converter becomes a three-level wave while the other is a two-level 50 % square wave. By enabling a time interval of which the voltage is zero in the three-level voltage, the power flow in that time interval will be zero and thus the circulating power is decreased.

Compared to the SPS control, the EPS features several advantages such as; reduced current stress, enhances regulating flexibility, improves efficiency and expands the soft switching operation range. [23]

Dual phase-shift control (DPS)

To further improve the SPS control for the isolated DC/DC converter, [32] proposed a dual phase-shift control scheme which is aiming to increasing system power capability and eliminating reactive power. Compared to the more traditional SPS control, the DPS control has many advantages such as; limit inrush current, decrease peak current, minimized output capacitance, eliminate reactive power and increased system efficiency [31]. DPS control also enables improved modulation strategy which allows for soft-switching operation in the entire power range.

Similar to the EPS control, the DPS control uses an inner phase-shift angle. But the difference between those two is that DPS uses an inner phase-shift angle for both bridges. Compared to the EPS control, the operating states of the two bridges are the same if the power flow direction or voltage conversion states are changed. This makes the DPS control easier to implement and the dynamic performance may be better. [23]

Triple phase-shift control (TPS)

TPS control is similar to DPS control. As in DPS, an inner phase-shift angle is used for both bridges but in TPS they can be controlled independently. This creates a third degree of control freedom.

Different control schemes using TPS control has been investigated in several research papers, such as [33] and [34], and they have all different goals and possible advantages.

All the different control schemes show improved soft-switching region during zero-load condition, reduced peak and RMS currents and a significant reduction in the size of the isolation transformer. [33] [34]

The TPS control was in fact proposed after SPS, EPS and DPS control were proposed, unifying the phase-shift control. SPS, EPS and DPS control can also be regarded as a special case of TPS control.

From an implementation view, SPS control requires one degree of control; EPS and DPS requires two degree of control, and TPS requires three degrees. This implies that TPS control strategy is most difficult to implement in a control scheme and additionally there is no unified standard for the TPS control at the moment. [23]

The proposed modularized dual active bridge utilizes the modular configuration to enable low voltage switches which reduces power losses and possibly converter volume. By using a modular design, a different control scheme needs to be implemented in order to utilize the modular configuration in the best possible way.

The proposed control scheme for the modular configuration only uses one distributed voltage loop to realize both output current sharing and input voltage, possible high-level fault tolerance, plug-and-play capability and easy implementation. The control scheme consists of a simple SPS control which uses the output voltage of each module for controlling the output voltage of the converter. [35]

Moreover, another advantage of the modular control scheme for the proposed input-series-output-parallel (ISOP) configured converter is that the power rating of the converter can easily be expanded by connecting several ISOP configured converters in an input-parallel-output-parallel (IPOP) while no additional control system is required [35]. This means that ISOP converters can be configured for a specific power rating, for example 50 or 100 kW, and then connected in IPOP to meet the specific load requirement of the equipment. This may lead to lower design and manufacturer cost due to the fact that only one converter needs to be designed for several purposes.

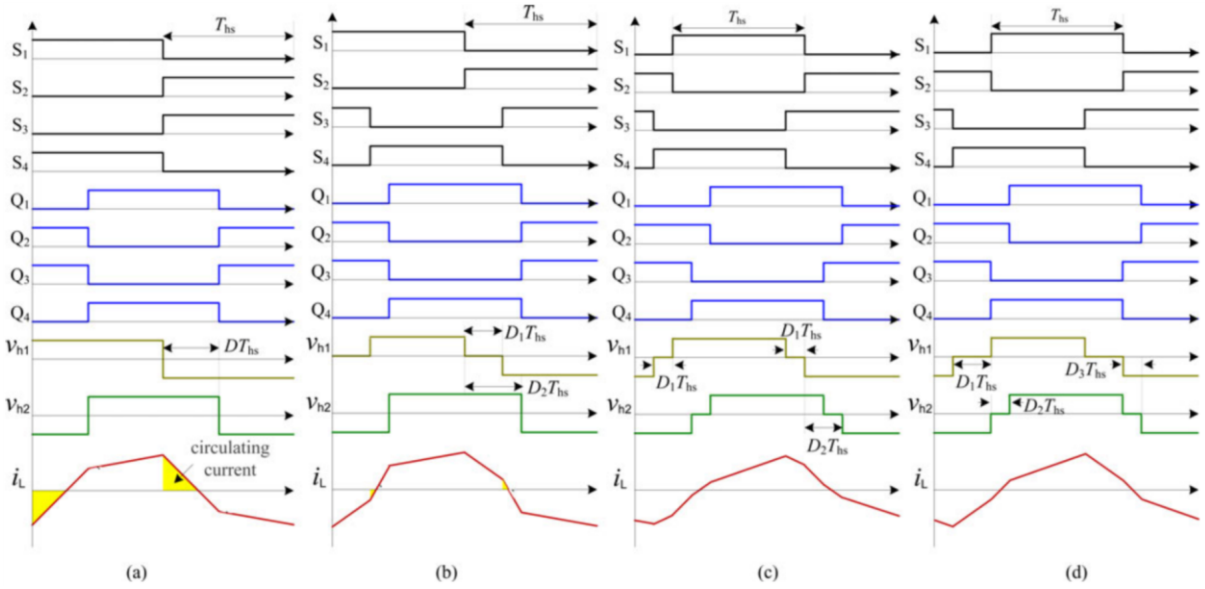

Figure 3.10: (a) SPS control (b) EPS control (c) DPS control (d) TPS control [23]

4 Converter design

The DAB and MDAB converters presented in chapter 3 will be designed and compared for different voltage levels. Since the input voltage is not clear at this point, several voltage levels will be considered for each converter. The converters will be designed for a power rating of 100 kW. One of the most important design criteria for the ROV application is to have low volume and weight. Converter efficiency is a second priority. However, the converter efficiency should still be decent.

The DAB converter is chosen for its high power density, high efficiency, simple design, high reliability and it's all active switch design. While the diodes in the SAB and the additional capacitors in the DHB may lead to an increased volume both for the additional capacitor requirements, the DAB uses active switches for both bridges in the converter. This leads to a more compact converter with a high power density. The 3ph-DAB could also a good alternative as the currents will be lower due to the additional phase. But since the currents for the ROV application are low and volume increasing solution such as parallel connection of switches is not needed, the 3ph-DAB may lead to higher volume both for the switching devices and for the transformer.

The MDAB is also chosen for its interesting modular design. As previously discussed, the modular advantages could be beneficial for the ROV application. By utilizing the modular design to obtain a higher switching frequency, the volume could be decreased significantly. The MDAB will be designed with modules using the DAB design.

For both the DAB and MDAB converter, the capacitance is of high importance. For the ROV application the converter volume must be as low as possible and since the capacitors are big and bulky, the capacitance must be minimized. Since the capacitance is related to the switching frequency, a high frequency is desired for the converter design.

Switches

The converter will be designed with commercially available components. This means that for the switching devices, IGBTs and low voltage SiC MOSFETs and GaN transistors can be used. Table 4.1 shows the data for the IGBT for different voltage levels. Table 4.3 shows data for the SiC MOSFETs for different voltage levels and table 4.2 shows data for different GaN transistors.

Due to the switching overvoltage, each switch will be dimensioned for 2/3 of the rated voltage. If a snubber circuit is used, the design voltage may be higher for each switch, but since a low volume converter is desired the snubber circuit will not be used for this thesis.

The free-wheeling diode in the converter design are not single components. Because the ROV application requires low volume and weight, the diode is included in the same package as the IGBT. For the SiC MOSFETs, the intrinsic body diode can be utilized during the blanking times, and after these the channels of the MOSFET can conduct the reveres current. By using the intrinsic body diode as free-wheeling diodes in the converter may lead to a lower efficiency. However, this is acceptable for the ROV design.

For the GaN transistor, there is no need for a parallel body diode as the transistors can conduct in 3rd quadrant without external anti-parallel diode. [36]

The volume of each switch has been calculated from the widest and highest point on the component.

Table 4.1: IGBT data for converter design (all data for 25°C) [37] [38] [39] [40]

	1.2 kV	**3.3 kV**	**4.5 kV**	**6.5 kV**	
Manufacturer	Infineon	Infineon	Powerex	Infineon	
Type	FZ400R12KS4P	FZ400R33KL2C_B5	QID4515004	FZ250R65KE3	
Device type	Single switch	Single switch	Phase leg	Single switch	
Isolation type	Si	Si	Si	Si	
Dimensioning voltage (2/3)	0.80	2.21	3.01	4.35	[kV]
$I_{C(NOM)}$	400	400	150	250	[A]
R_{ON}	0.50	0.37	0.80	0.36	[mΩ]
Turn-on time	0.10	1.00	1.00	0.70	[µs]
Turn-off time	0.53	3.70	3.60	7.30	[µs]
E_{ON}	22	900	550	1400	[mJ]
E_{OFF}	29	440	340	1200	[mJ]
L_{STRAY}	16	25	60	25	[nH]
Size (L x W x H)	106 x 61 x 36.5	140 x 73 x 48	140 x 73 x 38	140 x 73 x 48	[mm]
Volume	236.01	490.56	388.36	490.56	[cm^3]
Weight	0.34	0.50	0.80	0.50	[kg]

Table 4.2: SiC MOSFET data for converter design (all data for 25°C) [41] [42] [43]

	0.65 kV	**1.2 kV**	**1.2 kV**	
Manufacturer	ST	ST	ST	
Type	SCTW100N65G2AG	SCT20N120	SCT50N120	
Device type	Discrete	Discrete	Discrete	
Isolation type	SiC	SiC	SiC	
Dimensioning voltage (2/3)	0.43	0.80	0.80	[kV]
$I_{C(NOM)}$	100	20	65	[A]
R_{ON}	22	189	59	[mΩ]
Input cap.	3600	650	1900	[pF]
Output cap.	305	65	170	[pF]
E_{ON}	0.30	0.16	0.53	[mJ]
E_{OFF}	0.25	0.90	0.31	[mJ]
Max operating temp.	200	150	150	[°C]
Size (L x W x H)	15.5x19.9x4.9	15.5x19.9x4.9	15.5x19.9x4.9	[mm]
Volume	1.51	1.51	1.51	[cm^3]
Weight	Negligible	Negligible	Negligible	[kg]

Table 4.3: GaN Transistor data for converter design (all data for 25°C) [44] [45] [46]

	0.65 kV	**0.65 kV**	**0.65 kV**	
Manufacturer	GaN Systems	GaN Systems	GaN Systems	
Type	GS66504B	GS66508B	GS66516B	
Device type	Discrete	Discrete	Discrete	
Isolation type	GaN	GaN	GaN	
Dimensioning voltage (2/3)	0.43	0.43	0.43	[kV]
$I_{C(NOM)}$	15	30	60	[A]
R_{ON}	100	50	25	[mΩ]
Input cap.	130	260	520	[pF]
Output cap.	33	65	130	[pF]
Max switch. freq.	>10	>10	>10	[MHz]
Size (L x W x H)	5.0x6.6x0.5	7.1x8.5x0.56	11x9.0x0.54	[mm]
Volume	0.0165	0.0338	0.0535	[cm^3]
Weight	Negligible	Negligible	Negligible	[kg]

Capacitors

The converters always need capacitors in their input and output stage to lower the voltage ripple. The capacitors must tolerate high pressure. As seen in [18] and [47], the aluminum electrolytic capacitor can have small air pockets inside the wound construction. This can cause deformation of the material and eventually short-circuits. Another alternative is ceramic capacitors. They are very small in size and can be designed to withstand high voltage. However, they are not capable of handling high currents. The ceramic capacitors have huge compressive strength and can sustain long lifetime in a high-pressure environment. The ceramic material is more fragile than the electrolytic capacitors and can break when subjected to many pressure cycles during operations. Polypropylene (PP) film capacitors is another alternative. They are big in size, but they have long estimated lifetime, low equivalent series resistance (ESR) and has proven to tolerate high pressure during tests [18]. Table 4.4 shows data for PP film capacitors from VISHAY. These capacitors will be used for designing the converters in this thesis.

Table 4.4: Capacitor data for converter design [48]

	0.63 kV	**0.63 kV**	**1.25 kV**	**1.25 kV**	
Manufacturer	VISHAY	VISHAY	VISHAY	VISHAY	
Type	MKP385	MKP385	MKP385	MKP385	
Device type	PP film	PP film	PP film	PP film	
Capacitance	3.3	6.2	3.3	5.1	[µF]
I_{rms}	17.0	27.0	33.0	35.0	[A]
ESR	3.0	3.0	2.0	5.0	[mΩ]
Size (W x H x L)	18 x 32.5 x 41.5	24 x 44 x 42	25 x 45 x 57.5	35 x 50 x 57.5	[mm]
Volume	24.28	44.35	64.69	100.63	[cm^3]
Weight	0.029	0.050	0.100	0.150	[kg]

4.1 Dual active bridge (DAB)

The dual active bridge is chosen for its well proven design. It is equipped with four switches in its two bridges. The bridges are connected to each other through a high frequency transformer which both creates the galvanic isolation and transforms the voltage to a desired level. An inductor is needed for the power transfer and should be placed in series with the transformers primary winding. The inductor is often embedded into the design of the transformer to further lower the volume and weight of the converter. Capacitors are needed for the output stage of the converter to lower the voltage ripple.

Switches

For the DAB converter, the rated input voltage will be put through each switch in the primary bridge. That is why IGBTs is the natural selection for the primary switches. The number of IGBTs on the input side of the converter is based on the converter voltage design. Since one of the most important criteria when designing power electronic converters for ROV application is volume and weight, an effort to minimize the number of switches has been made. For the converters designed for a higher voltage than the IGBTs rated blocking voltage, two or more IGBTs must be series connected to obtain a higher blocking voltage. This may lead to higher complexity of the converter and control design, but the added complexity is not considered in this thesis.

For the output stage of the converter, a voltage of 0.7 kV has been chosen and therefore the 1.2 kV IGBT is chosen as the output switch for all different input voltage levels.

Table 4.5: Switching device selection for the DAB converter

Converter voltage design	**3.0/0.7 kV**	**4.5/0.7 kV**	**6.0/0.7 kV**	**10/0.7 kV**	**15/0.7 kV**
Switch type primary side	4.5 kV 150 A	3.3 kV 400 A	4.5 kV 150 A	6.5 kV 250 A	6.5 kV 250 A
No. of switches primary side	4	8	8	12	16
Switch type secondary side	1.2 kV 400 A	1.2 kV 400 A	1.2 kV 400 A	1.2 kV 400 A	1.2 kV 400 A
No. of switches secondary side	4	4	4	4	4
Total volume	2.497 dm^3	4.868 dm^3	4.050 dm^3	6.830 dm^3	8.793 dm^3
Total weight	4.56 kg	5.36 kg	7.76 kg	7.36 kg	9.36 kg

The output voltage from the DAB converter will need filtering to stay within the ripple limits. An attempt to calculate the capacitance was made before these values were tested and adjusted during converter simulation.

The highest voltage ripple will occur at the lowest power output. As stated in chapter 3, the lowest power output is 200 W. Therefore, in the simulation, the load is set to 200 W.

Figure 4.1 shows the capacitance necessary to maintain 10 % ripple on the output voltage related to the switching frequency. The table is produced from simulation results as described in chapter 5. As expected at low switching frequencies, the capacitance is very high and at higher frequencies the capacitance is significantly reduced.

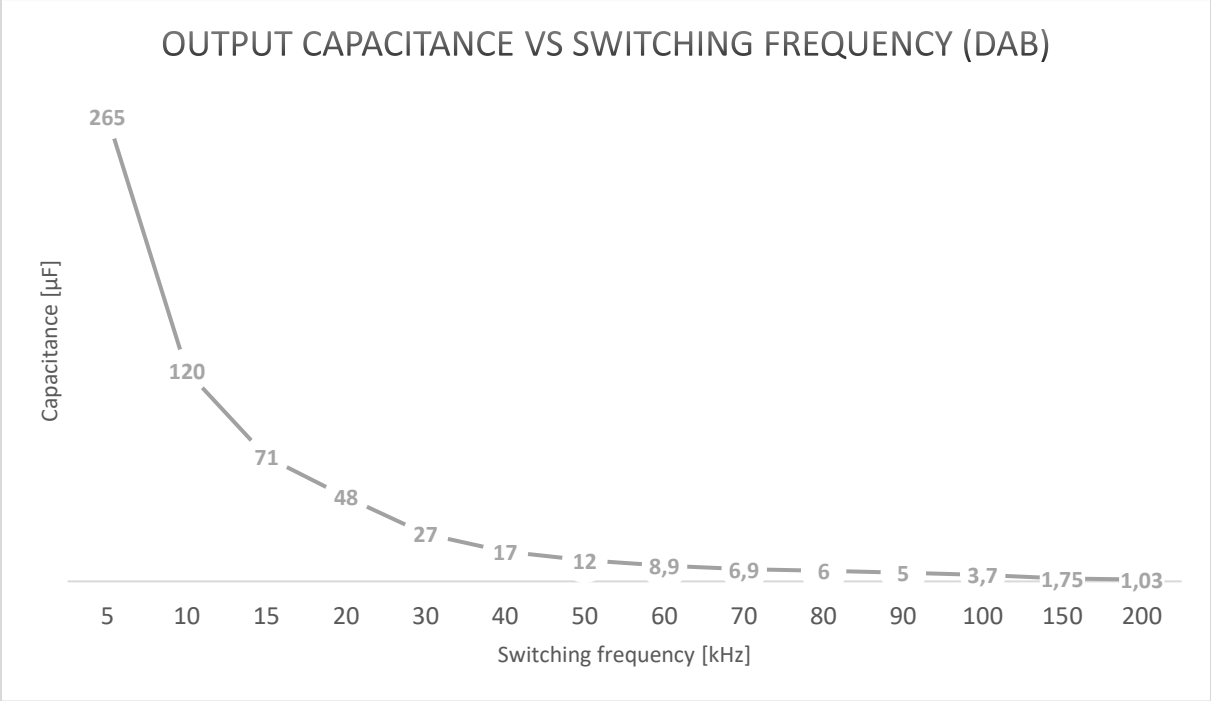

Figure 4.1: Output capacitance vs switching frequency from simulation for DAB converter to maintain 10 % ripple

Figure 4.2 shows as expected the same pattern as figure 4.1. The capacitor volume will decrease when higher frequency is applied. By increasing the frequency from 5 to 15 KHz, the volume is reduced by almost 75 %. By further increasing the frequency, at 50 KHz the volume is reduced by approximate 95 % from 5 KHz.

This reduction in capacitance happens due to the increase switching frequency. From the formula shown below, it is clear that by increasing the switching frequency, while maintaining the output voltage and ripple at the same level, the capacitance will decrease.

$$C_{out} = \frac{I_{out} \cdot DT_s}{V_{out} \cdot V_{ripple(\%)}} = \frac{142 \cdot 0.5 \cdot \frac{1}{15000}}{700 \cdot 0.1} = 67.6\ \mu F \quad 4.1$$

$$C_{out} = \frac{I_{out} \cdot DT_s}{V_{out} \cdot V_{ripple(\%)}} = \frac{142 \cdot 0.5 \cdot \frac{1}{50000}}{700 \cdot 0.1} = 20.28\ \mu F \quad 4.2$$

The calculated values are theoretical values and may not be accurate for real-life application. In order to find the correct value, these capacitance are simulated in Simulink, and then adjusted to find the correct value for an output voltage ripple of 10 %.

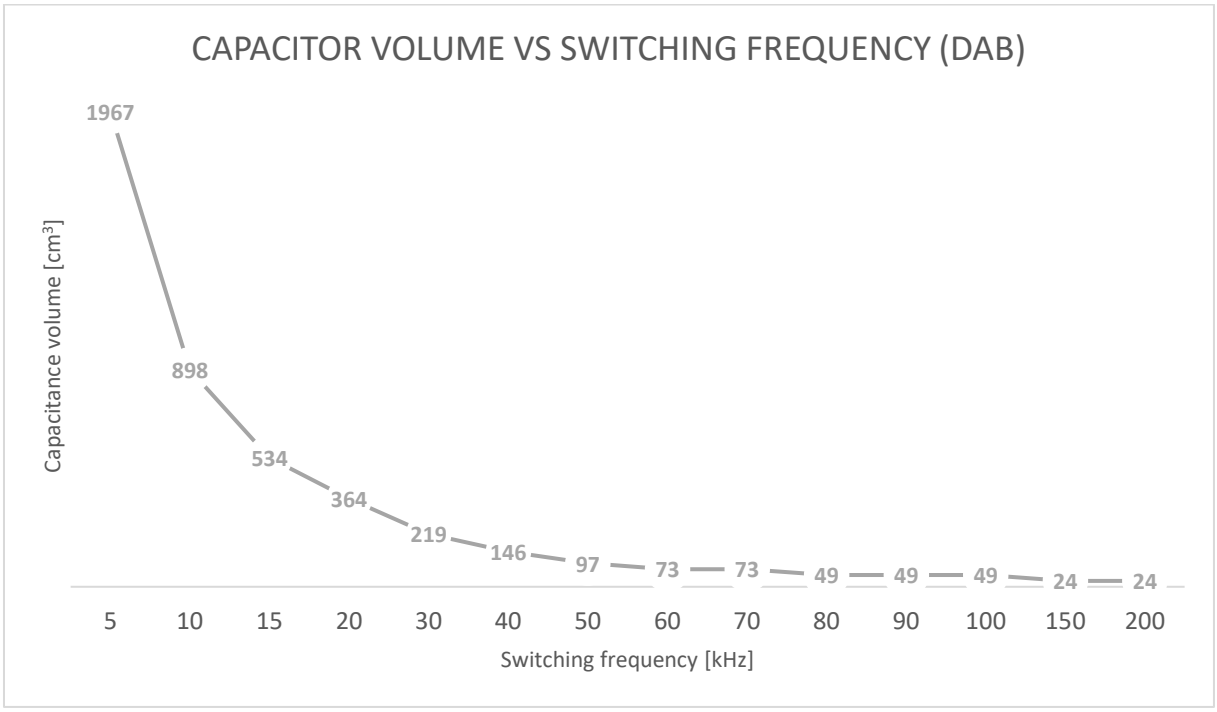

Figure 4.2: Capacitance volume vs switching frequency for DAB converter

It should also be mentioned that the capacitance is highly dependent to the tuning of the control system for the converter. By further tuning the control parameters or using a different control strategy, lower output capacitance may be achieved.

Transformer and inductor

The high-frequency transformer is one of the key component for the DAB, which has direct impact on the performance [23]. However, the design of the transformer is out of scope for this thesis. The transformer will use data previously shown in table 3.3. The ABB transformer will be scaled to 100 kVA as shown in table 4.6. The scaling is done by using the power density for the original transformer and calculating the power density for the 100 kW used in this thesis. The scaling of voltage and switching frequency is not relevant for the purpose of volume estimation.

Table 4.6: Transformer values scaled for DAB converter

Condition	**Symbol**	**Values** [19]	**Scaled values**
Rated power	P_N	350 kVA	100 kVA
Primary voltage	V_{PRMS}	3000 V	3 - 15 kV
Secondary voltage	V_{SRMS}	3000 V	0.7 kV
Switching frequency	f_{sw}	10 kHz	5-15 kHz
Weight		< 50 kg	14.3 kg
Volume		37 dm^3	10.5 dm^3
Power density		9.5 kVA/dm^3 - 7 kVA/kg	9.5 kVA/dm^3 - 7 kVA/kg

Converter volume and weight

The total volume of the converter is difficult to estimate. There are several components which isn't evaluated in this thesis. The gate drivers and control boards are not considered. For the DAB converter, each switch will have a circuit board that contains the gate driver, power supply, control circuitry and some small filters. The added volume from the circuit board may lead to a small increase in volume. As shown in figure 4.3, the two main contributors to the total converter volume is the IGBTs and transformer. Since this thesis uses a generic transformer which is not designed for the ROV application, it may be possible to have a different design to meet the design requirements for the ROV application.

The lowest volume is obtained when using the lowest voltages. 3.0/0.7 kV gives a volume of 15 dm^3 for 5 kHz and 13.5 dm^3 for 15 kHz. Because the IGBT devices used for the lowest voltages have a lower voltage rating, their packaging will also be lower in volume compared to the higher rated IGBTs. The highest rated IGBTs will be bulkier because the creeping distance must be longer due to the higher voltage rating.

Also when the output voltage is kept at the same level, there is no difference in the output capacitance for the different voltage level. As observed, the capacitance is only reduced when the switching frequency is increased.

6.0 kV may be a good alternative if a higher voltage is desired as it only increases the size of 1.5 dm^3 for all three frequencies. 15 kV gives the highest volume as it needs a total of 16 devices of 6.5 kV IGBTs in the primary bridge. The volume is increased by over 6 dm^3 for all frequencies which is an increase of approximate 41 % compared to the lowest voltage.

The IGBTs and transformer is also the dominate contributors to the weight. The capacitors have negligible weight compared to the IGBTs and transformer. For a 100 kW transformer with a 7 kVA/kg power density the weight will be approximate 14.3 kg. The IGBTs will contribute to a weight between 4.5 – 9.4 kg depending on the voltage design. The circuit boards for the converter will add some weight, but it is negligible compared to the IGBTs and transformer. The total weight of the converter will be approximate 18.8 – 23.7 kg.

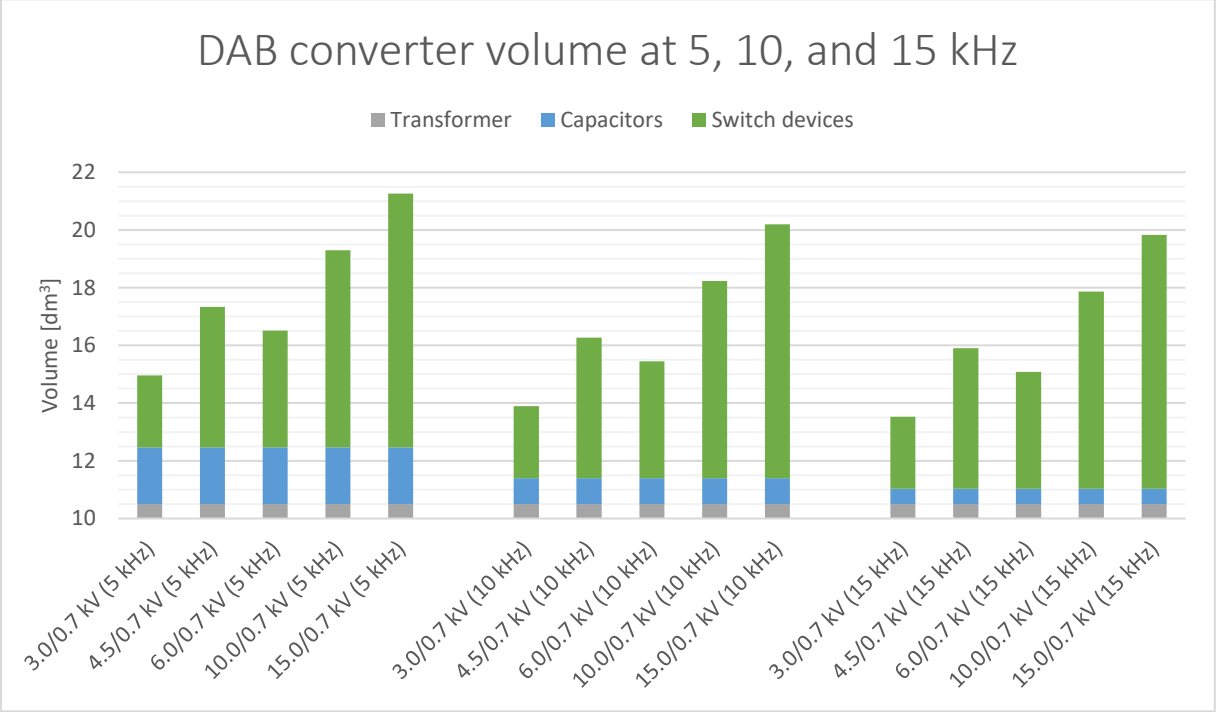

Figure 4.3: DAB converter volume at 5, 10 and 15 kHz for different voltage levels

4.2 Modularized dual active bridge (MDAB)

The modularized dual active bridge consists of several DAB converters connected in a modular configuration. For the ROV application it is beneficial to decrease the input voltage over each switching device and to have a higher switching frequency to decrease the volume of the passive components. This can be achieved by series connecting the input, and parallel connecting the output.

Modular configuration

One of the great advantages with the MDAB is the modular configuration which enables low voltage switching devices. The number of modules decides the voltage level of each device and their current rating. To achieve a low enough voltage over each device, the input voltage must be divided in a proper number of modules. For the 0.65 kV device, the maximum applied voltage would be approx. 0.43 kV. For the 1.2 kV device, the maximum voltage would be approx. 0.8 kV. This means in order to use the 0.65 kV devices for an input voltage of 3 kV, there must be at least 7 modules in the converter. And for the 1.2 kV devices, at least 4 modules are needed. For an input voltage of 4 kV, 10 modules of 0.65 kV devices or 5 modules of 1.2 kV devices are needed. An input voltage of 6 kV gives 14 modules for the 0.65 kV devices and 8 modules for the 1.2 kV devices.

This thesis has investigated a 10 module MDAB for easier comparison between each voltage and device configuration. Table 4.7 shows the dimensioning input and output current for each module in a 10 module MDAB.

Table 4.7: Current per module for the 10 module MDAB

Converter voltage design	**3.0/0.4 kV**	**3.0/0.7 kV**	**4.0/0.4 kV**	**4.0/0.7 kV**	**6.0/0.7 kV**	
Input current per module	3.3	3.4	2.5	2.5	1.7	[A]
Output current per module	25.0	14.3	25.0	14.3	14.3	[A]

Switches

For the MDAB the voltage through each switch is the applied voltage divided by the number of modules. This means that low voltage Silicon Carbide MOSFETs and Gallium Nitride transistors can be used. These devices offer the capability of faster switching times, lower conduction losses and overall better performance.

Table 4.8 and table 4.9 shows a possible device selection for SiC and GaN devices.

Table 4.8: SiC device selection per module for the 10 module MDAB

Converter voltage design	3.0/0.4 kV	3.0/0.7 kV	4.0/0.4 kV	4.0/0.7 kV	6.0/0.7 kV
Switch type primary side	0.65 kV 100 A	0.65 kV 100 A	1.2 kV 20 A	1.2 kV 20 A	1.2 kV 20 A
No. of switches primary side	4	4	4	4	4
Switch type secondary side	0.65 kV 100 A	1.2 kV 20 A	0.65 kV 100 A	1.2 kV 20 A	1.2 kV 20 A
No. of switches secondary side	4	4	4	4	4
Total volume	12.08 cm^3	12.08 cm^3	12.08 cm^3	12.08 cm^3	12.08 cm^3
Total weight	Negligible	Negligible	Negligible	Negligible	Negligible

Table 4.9: GaN device selection per module for the 10 module MDAB

Converter voltage design	3.0/0.4 kV	3.0/0.7 kV	4.0/0.4 kV	4.0/0.7 kV	6.0/0.7 kV
Switch type primary side	0.65 kV 15 A	0.65 kV 15 A	0.65 kV 15 A	0.65 kV 15 A	0.65 kV 15 A
No. of switches primary side	4	4	4	4	8
Switch type secondary side	0.65 kV 30 A	0.65 kV 30 A	0.65 kV 30 A	0.65 kV 30 A	0.65 kV 30 A
No. of switches secondary side	4	8	4	8	8
Total volume	0.20 cm^3	0.30 cm^3	0.20 cm^3	0.30 cm^3	0.40 cm^3
Total weight	Negligible	Negligible	Negligible	Negligible	Negligible

Capacitors

The output voltage from the MDAB converter will need filtering to stay within the ripple limits of 10 %. An attempt to calculate the capacitance was made before these values were tested and adjusted during converter simulation.

The highest voltage ripple will occur at the lowest power output. As stated in chapter 3, the lowest power output is 200 W. Therefore, in the simulation, the load is set to 200 W.

Figure 4.4 shows the capacitance necessary to maintain 10 % ripple on the output voltage related to the switching frequency. The table is produced from simulation results as described in chapter 5.

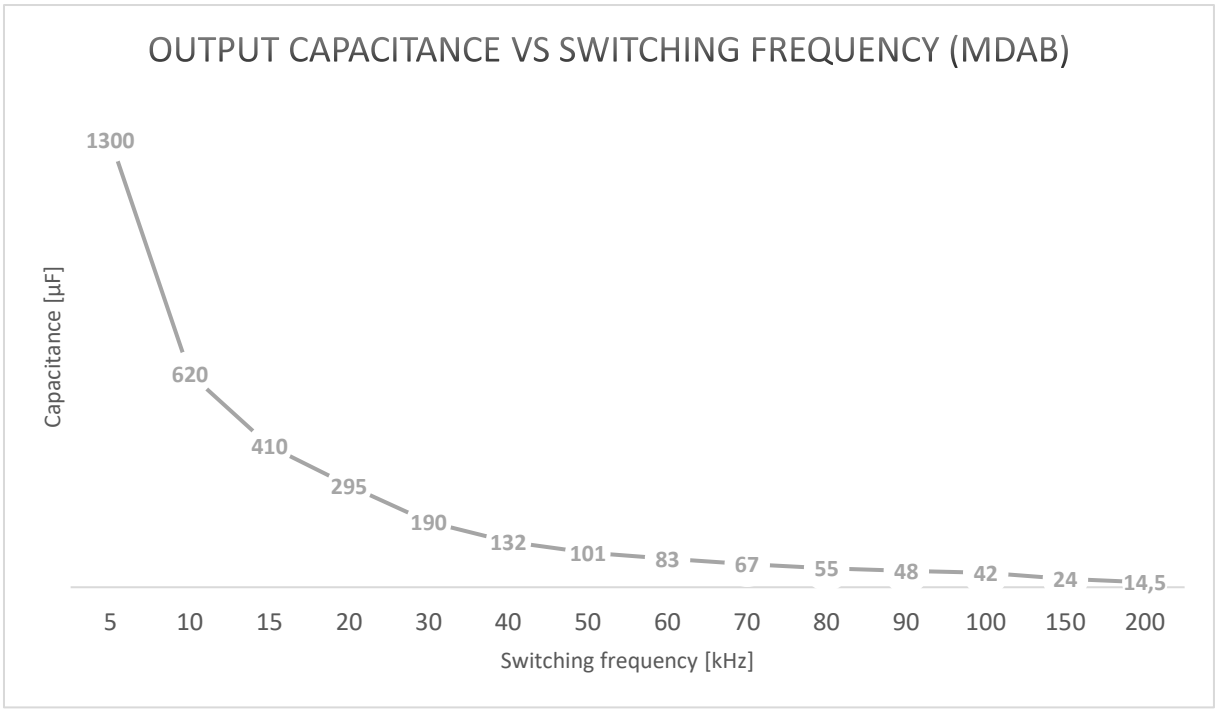

Figure 4.4: Total output capacitance vs switching frequency from simulation for MDAB converter

By increasing the switching frequency from 5 to 15 kHz, a reduction of approx. 70 % is achieved. By further increasing the frequency to 50 kHz, the reduction is increased to approx. 92 % from 5 kHz. If the switching frequency is increased to 100 kHz, the capacitance is decreased by approx. 97 %.

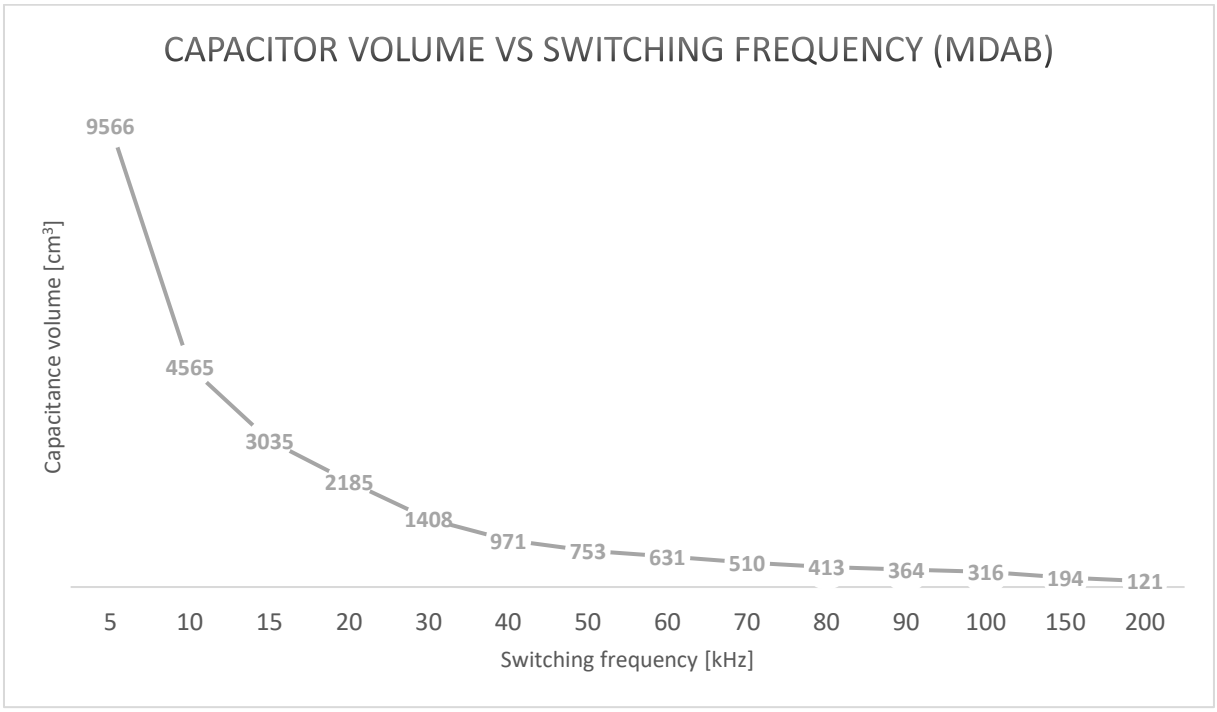

Figure 4.5: Total capacitance volume vs switching frequency for MDAB converter

Transformer and inductor

The high-frequency transformer is one of the key component for the DAB modules, which has direct impact on the performance [23]. However, the design of the transformer is out of scope for this thesis. The transformer will use data previously shown in table 3.5. The Vtech transformer will be scaled to 100 kW as shown in table 4.10. The scaling is done by using the power density for the original transformer and calculating the power density for the 100 kVA used in this thesis. The scaling of voltage and switching frequency is not relevant for the purpose of volume estimation.

Table 4.10: Transformer values scaled for MDAB converter

Condition	**Symbol**	**Values** [21]	**Scaled values**
Rated power	P_N	30 kW	100 kVA
Primary voltage	V_{PRMS}	280 - 325 V	400 - 700 V
Secondary voltage	V_{SRMS}	10 000 V	3 - 15 kV
Switching frequency	f_{sw}	79 - 200 kHz	20 - 200 kHz
Weight (estimated)		3 kg	10 kg
Volume		1.71 dm^3	5.71 dm^3
Power density		17.5 kW/dm^3 - 10 kW/kg	17.5 kW/dm^3 - 10 kW/kg

Converter volume and weight

The total volume of the converter is difficult to estimate. There are several components which aren't evaluated in this thesis. The gate drivers and control boards are not considered. For the MDAB, each module will have a circuit board that contains the gate driver, switches, inductor and transformer as shown in [29]. The added volume from the circuit board may lead to a substantial increase in volume. As shown in Figure 4.6, the main contributor to the total converter volume is the transformer. Since this thesis uses a generic transformer which is not designed for the ROV application, it may be possible to have a different design to meet the design requirements for the ROV application.

Figure 4.6 shows the total converter volume for switching frequencies of 15, 50, 100 and 200 kHz. 15 kHz is considered a medium frequency and it's only included for comparison purpose of the higher frequencies. The medium frequency transformer, shown in table 4.6, is also used in the volume calculations for 15 kHz. As observed in figure 4.6, the volume for the 15 kHz converter is very high compared to the higher frequencies, and it will not be a reasonable alternative for the MDAB.

As seen in table 4.8 and table 4.9, the input voltage does not affect the volume of the switches for SiC and GaN. They are the same for the entire voltage range. It should be mentioned that if higher voltages are desired, several devices need so be series connected leading to a higher volume. Nevertheless, the increased volume may have negligible effect on the total volume.

Compared to 15 kHz, the design for 50, 100 and 200 kHz will be significant lower. For 50 kHz the total volume is reduced by over 50 %. For 200 kHz the reduction is more than 56 %. It is also observed that

the difference in volume from 50 kHz to 200 kHz is small. There is a difference of 0.75 dm^3, which is approximate 11 % of the total volume.

The transformer is also the dominate contributor to the weight. The switching devices and capacitors has negligible weight. For a 100 kW transformer with a 10kW/kg power density the weight will be approximate 10 kg for the 50, 100 and 200 kHz converter. The circuit boards for the converter will add some weight, but it is probably negligible compared to the transformer.

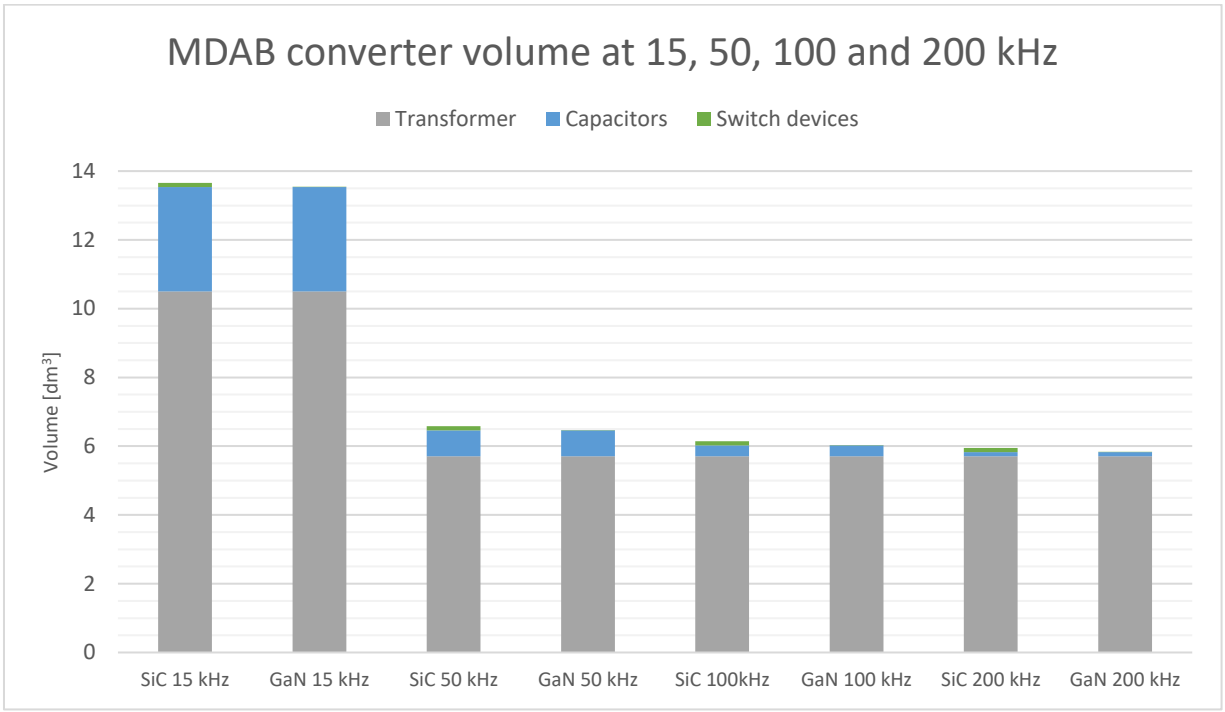

Figure 4.6: MDAB converter volume at 50, 100 and 200 kHz for different voltage levels

5 Simulation

To determine the performance and validity of the calculated components, the converters are simulated in the MathWorks MATLAB/Simulink software. Although power electronic components introduce several benefits to the system, regarding control and conversion in the system, it may also introduce a more complex system as a result of semiconductor devices with switching characteristics [49]. This leads to a system which is complex and contains both electrical and mechanical components with very different characteristics. Mechanical time constants for hydrodynamics can be in several seconds, while power electronic components can have a time constant in the range on nanoseconds. Creating a simulation model for the entire electrical and mechanical system with all of its components can be challenging. Therefore in this thesis, only the power electronic converters have been simulated in a simplified model. The details of the converter simulation models are discussed in the following chapters.

5.1 Dual active bridge simulation model

The dual active bridge has been simulated as shown in figure 5.1. A DC voltage source feeds the converter with the proper input voltage. The inductor is tuned to fit the voltage, current and switching frequency by using the inductor formula. The transformer parameters are set to the values of the ABB transformer listed in table 3.3. The load resistance is calculated to meet the desired output power and there has also been implemented step change in output power during simulation. Figure 5.1 shows a simplified model of the DAB converter in Simulink.

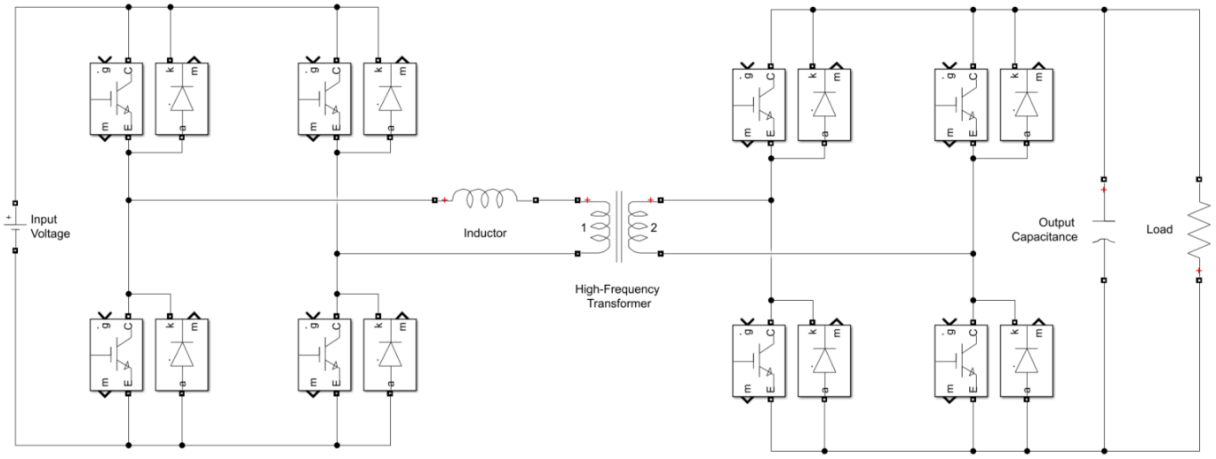

Figure 5.1: Dual active bridge Simulink model

Inductor parameter

For this thesis the main objective is not to fine tune the inductor parameters. However, an inductance needs to be calculated in order to have a proper performance for the simulation. The inductance calculation is shown in equation 5.1. The calculated parameters used in the simulation model is listed in Appendix B – Tables.

$$L_{boost} = \frac{V_{out} \cdot DT_s}{I_{out}} \tag{5.1}$$

Capacitance calculation

In order to have an approximate capacitance for the simulation, the capacitance needs to be calculated. The calculated value is put into the simulation model and then tuned to the meet the desired output voltage ripple. The capacitance calculation is shown in equation 5.2. The calculated parameters used in the simulation model is listed in Appendix B – Tables.

$$C_{out} = \frac{I_{out} \cdot DT_s}{V_{out} \cdot V_{ripple(\%)}} \tag{5.2}$$

Output resistor

During simulation the load must be set to a proper value. As described in chapter 3, the minimum load during ROV operation is approximate 200 W. This leads to a resistance of 2450 ohm for an output voltage of 700 V. The calculation is shown in equation 5.3. As previously mentioned the converter has also been simulated with a step change in the load. The output power is set to 50 % and 100 % during simulation to verify the function of the control system and the calculated parameters.

$$R_{load} = \frac{V_{out}^2}{P_{out}} \tag{5.3}$$

Tuning of control system

The control system for the converter is chosen to be a single phase-shift control (SPS). The SPS control scheme is very easy to implement and provides good performance for the DAB converter. Due to the fact that the purpose of this thesis is to find the optimal converter design for the ROV application, and not a control system thesis, the type and design of the control system can most certain be enhanced. If the control system is enhanced, the passive elements in the converter may have smaller parameters and thus smaller volume.

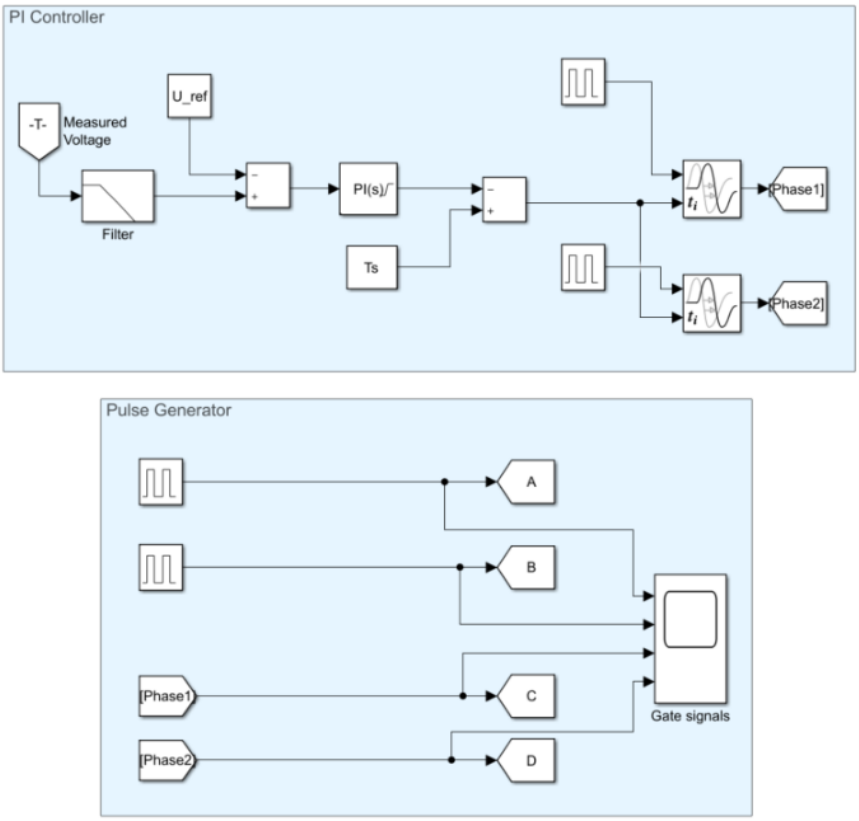

Figure 5.2: PI controller and pulse generator for the dual active bridge converter

The measured voltage is compared to the reference voltage and the error signal is then fed into the PI controller. The PI controller has a lower and upper limit of 0 - 90°, which corresponds to a time delay of minimum 0 seconds to a maximum of $T_s/4$ seconds. The time delay is fed into the gate signals for the second bridge. The parameters for the control system is shown in Appendix C – MATLAB script (DAB converter).

Simulation performance

As shown in figure 5.3, the SPS control system is functioning as expected. The output voltage is controlled to be 700 V. The figure shows that the simulation has been run with a step change in load for 0.2 kW – 50 kW – 100 kW. The output voltage is somewhat unstable at startup and load change but becomes stable after approximate 1 milliseconds at startup and 0.5 milliseconds after a load change. The PI controller could be optimized, but for this thesis the tuning is within scope.

At startup the voltage overshoots with approximate 125 V, which is almost 18 % of the reference voltage. At load change the transient voltage will be approximate 8.5 %. As expected the voltage ripple will be highest for the minimum load and lowest for the maximum load.

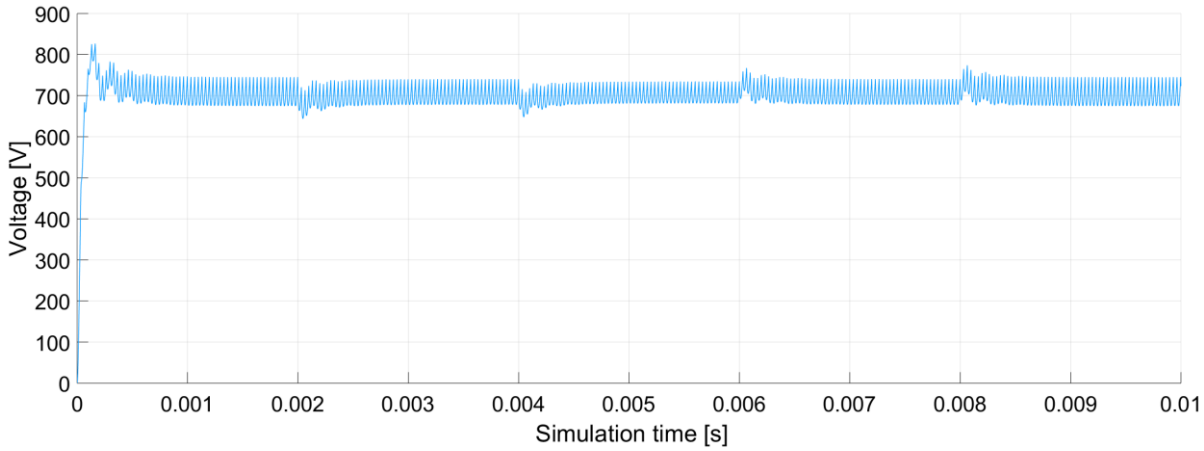

Figure 5.3: Simulation result for the output voltage of the DAB (f_{sw} = 15 kHz)

Figure 5.4 shows the current plot for the simulation. The first two milliseconds the outpower is set to 200 W, and the current is very low. The next two milliseconds the output power is increased to 50 kW and the current rises to approximate 71 A. Between four and six milliseconds the power is increased a second time to 100 kW which gives a current of approximate 142 A. After six milliseconds, the power is decreased at the same rate.

At load change the current will have almost no overshoot. The current is stable after approximate 0.5 milliseconds. As expected the current ripple will be highest for the maximum load and lowest for the minimum load.

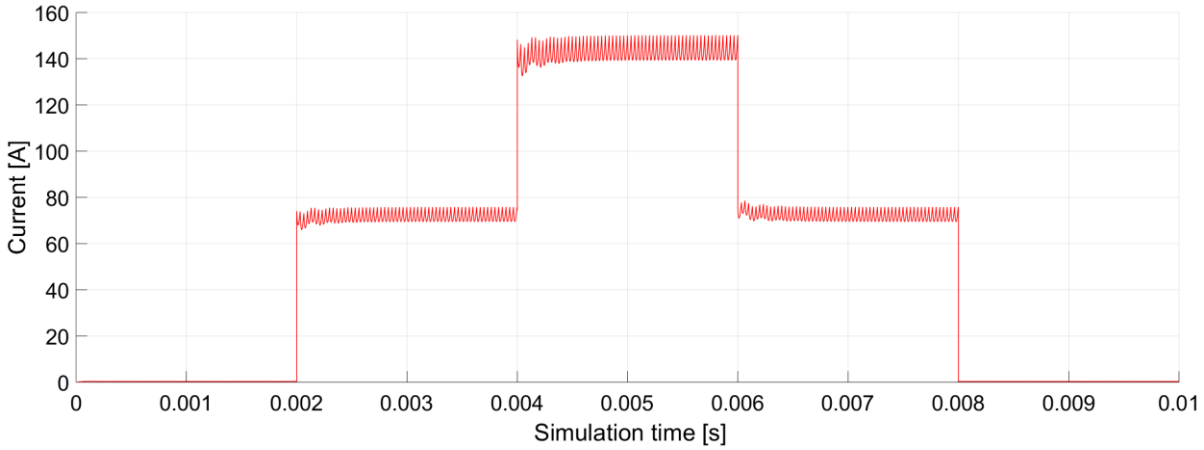

Figure 5.4: Simulation result for the output current of the DAB (f_{sw} = 15 kHz)

5.2 Modularized dual active bridge simulation model

The modularized dual active bridge is built up of several modules consisting of the DAB converter. For the Simulink simulation, the DAB converter presented in chapter 5.1 is used as modules. Each module has its own control system for the output voltage. Figure 5.5 shows the Simulink model of the MDAB.

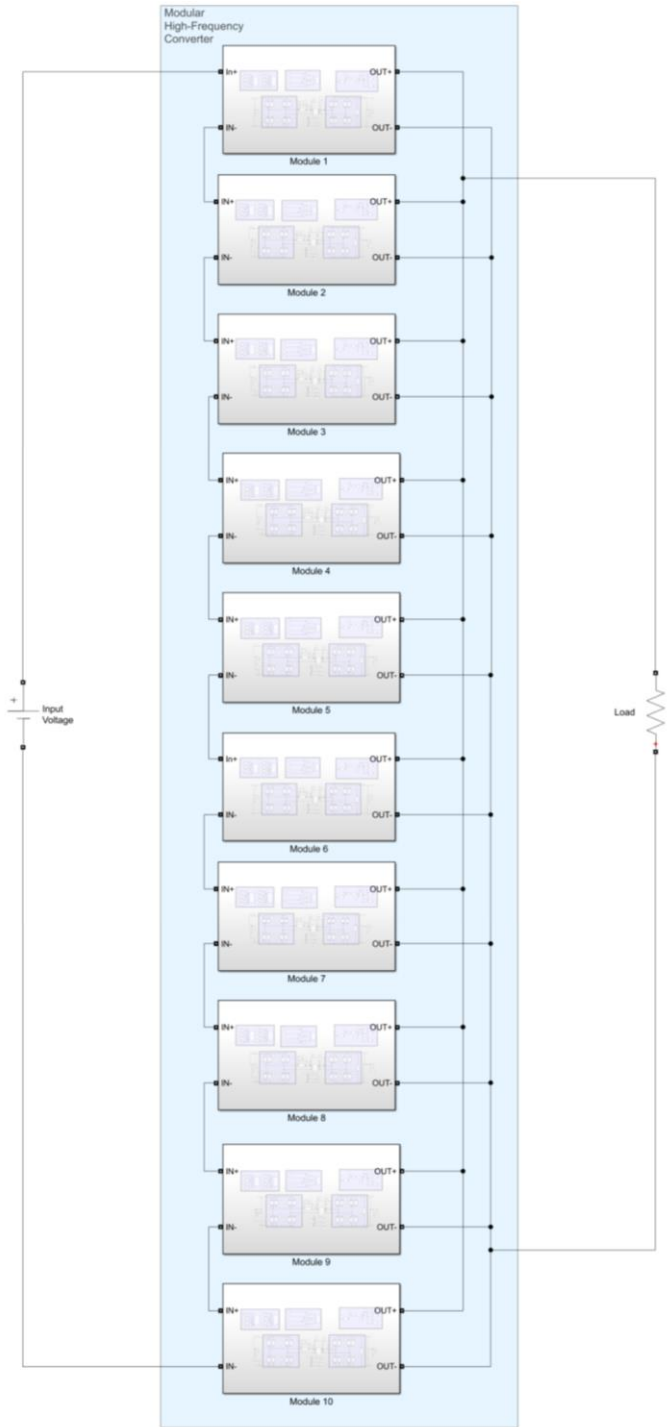

Figure 5.5: Module configuration for the modularized dual active bridge Simulink model

Inductor parameter

The inductance in the MDAB uses the same principle as the DAB converter. The total inductance needed is divided by the number of modules. The inductance calculation for each module is shown in equation 5.4. The calculated parameters used in the simulation model is listed in Appendix B – Tables

$$L_{boost} = \frac{V_{out} \cdot DT_s}{I_{out} \cdot n_{modules}} \quad 5.4$$

Capacitance calculation

In order to have an approximate capacitance for the simulation, the capacitance needs to be calculated. The calculated value is put into the simulation model and then tuned to the meet the desired output voltage ripple. The capacitance calculation for each module is shown in equation 5.5. The calculated parameters used in the simulation model is listed in Appendix B – Tables.

$$C_{out} = \frac{I_{out} \cdot DT_s}{V_{out} \cdot V_{ripple(\%)} \cdot n_{modules}} \quad 5.5$$

Output resistor

During simulation the load must be set to a proper value. As described in chapter 3, the minimum load during ROV operation is approximate 200 W. This leads to a resistance of 800 ohm for an output voltage of 400 V. The calculation is shown in equation 5.6. As previously mentioned the converter has also been simulated with a step change in the load. The output power is set to 50 % and 100 % during simulation to verify the function of the control system and the calculated parameters.

$$R_{load} = \frac{V_{out}^2}{P_{out}} \quad 5.6$$

Tuning of control system

The control system for the converter uses the same control system as for the DAB converter. Because the converter is parallel connected on the output, each module has its own PI controller which controls the output voltage of the module. The parameters for the control system is shown in Appendix D – MATLAB script (MDAB converter).

Figure 5.6 shows the simulation plots for the output voltage of the MDAB converter. The voltage is controlled to 400 V. As expected the voltage ripple will be highest for the minimum load and lowest for the maximum load. The converter has been simulated with a step loading of 0.2 – 50 – 100 kW.

At startup the voltage experiences no overshoot and has a very well-tuned control system. The voltage is stable at startup after less than 0.1 milliseconds. At a load change the converter has a transient voltage of approximate 6 % and is stable after 0.1 milliseconds.

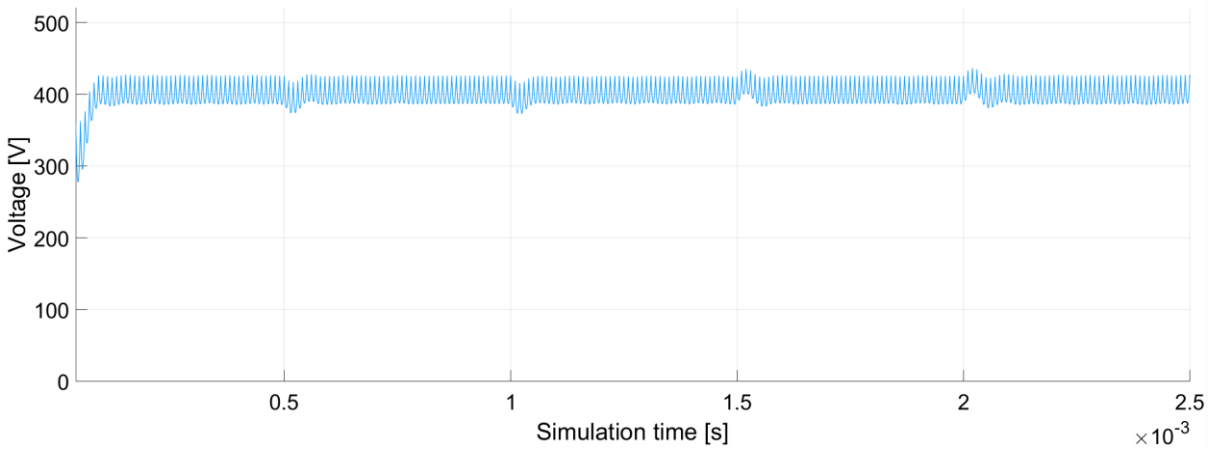

Figure 5.6: Simulation result for the output voltage of the MDAB (f_{sw} = 50 kHz)

For the current plot in figure 5.7, the current experiences a transient of approximate 4 % when the load is changed. The current in stable after 0.1 milliseconds. The first two milliseconds the outpower is set to 200 W, and the current is very low. The next two milliseconds the output power is increased to 50 kW and the current rises to approximate 125 A. Between four and six milliseconds the power is increased a second time to 100 kW which gives a current of approximate 250 A. After six milliseconds, the power is decreased at the same rate.

As the voltage plot, the current plot shows that the control system for the MDAB converter is very well-tuned. As expected the current ripple will be highest for the maximum load and lowest for the minimum load.

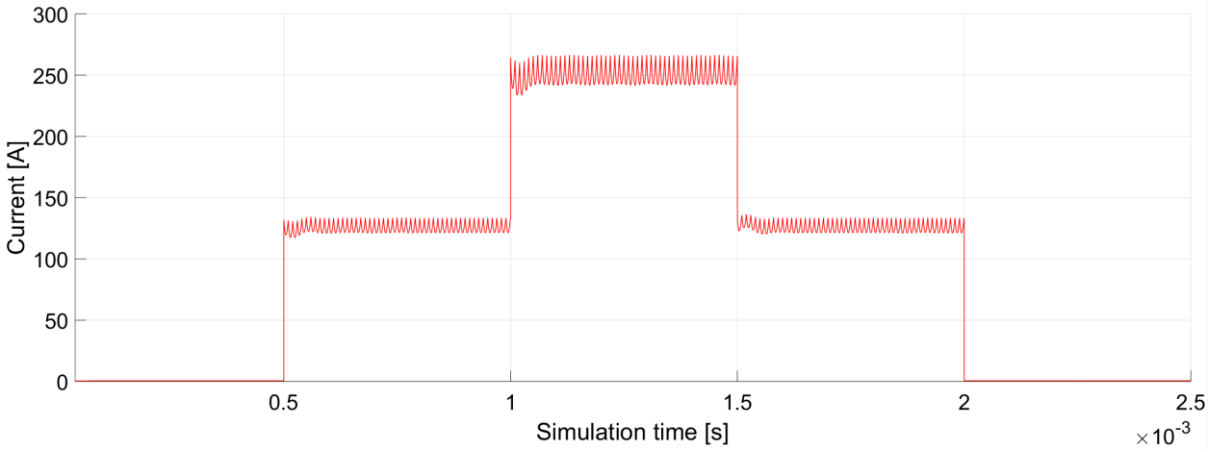

Figure 5.7: Simulation result for the output current of the MDAB (f_{sw} = 50 kHz)

6 Discussion

This thesis focuses on the idea of a fully electric work class ROV. The electrification of the work class ROVs may lead to several advantages such as lower maintenance, lower weight, thinner and lighter umbilical, smaller topside systems and a more environmental friendly design and operations. The literature study done previously to this thesis proposes a new electrical system utilizing a DC voltage throughout the ROV system. The ROV are fed with MVDC from the vessel trough the umbilical. The transmission voltage is proposed in the range of 3 – 15 kV DC. On the ROV a low voltage of 300 – 700 VDC are proposed. There are several benefits for using a MVDC for the ROV application, such as thinner and lighter umbilical, higher efficiency, smaller topside systems and a possible reduction in production and operation cost.

The literature study also identifies several challenges to the electrification. One of them are the voltage conversion for the ROV. By choosing power electronic converters over transformers, lower weight and volume may be achieved for the ROV. This thesis investigates different converter topologies to find a proper converter which can function as the main converter for the ROV.

Since the electrical system needs a galvanic isolation, isolated DC/DC converters are proposed. There are several different topologies available for an isolated DC/DC converter, and five of them which are most suitable for medium voltage and power design has been proposed in this thesis.

Two of the converters are chosen for further investigation; the dual active bridge and a modularized dual active bridge. The power rating of the converters is set to 100 kW.

The dual active bridge is a simple design using a simple control system. The converter is well known and has been used for many years in the industry. The designed DAB uses IGBTs as switching devices. Because the IGBT produce tail currents at turn-off the switching frequency is limited. The switching frequency is limited to maximum 15 kHz. Even lower frequencies may be preferred for the highest voltages and currents. A direct consequence for the limited switching frequency is the size of the passive components in the converter.

The total size of the designed DAB shows a volume of 13.5 – 21.0 dm^3 for the different voltages at a frequency of 15 kHz. This leads to a power density of 4.8 – 7.4 kW/dm^3. If the frequency somehow could be raised, the total volume most certain would be lowered considerably. In the future when high voltage SiC MOSFETs become available, the design of the DAB converter could be changed. Higher switching frequencies and higher input voltages may be realized. This could lead to a small and compact design for the DAB converter. But as of now, the IGBTs are the only real alternative for medium voltage inputs in a DAB converter.

The modularized dual active bridge has been proposed in several papers. It uses DAB modules which are series connected at the input, and parallel connected on the output. This connection utilizes switches which can operate at higher switching frequencies. Since the switches for the DAB converter is subjected to the full input voltage, the switches must be IGBTs. But if several modules could be series connected on the input, lower voltage would be applied to each switch. This leads to usage of low voltage switching devices which can have a considerably higher switching speed. By further using Silicon Carbide MOSFETs or Gallium Nitride transistors, the switching frequency could be raised to frequencies of 100 kHz and above. This leads to a substantial decrease of volume and weight for the passive components in the converter. The volume of the MDAB is calculated to be in the range of 5.8 – 6.6 dm^3 for switching frequencies of 50 – 200 kHz. This leads to a power density of 15.5 – 17.2

kW/dm^3. Since the converter uses discrete SiC or GaN devices, the input and output voltage will have very little impact on the total volume.

The modularized solution also comes with benefits for ROV manufacturers that produces several ROVs with different power ratings. By building MDAB converters with a specific power rating, several MDAB converters can be parallel connected to obtain higher power rating. This means that only one converter must be designed for all the manufacturers ROVs. This can reduce design and production cost as well as easier spare part logistics.

The volume is reduced by approximate 57 – 69 %, compared to the DAB, by choosing the MDAB converter depending on the voltage level. This is a great decrease in volume. It should however be mentioned that several components are not included in the volume calculations for either the DAB or MDAB such as the circuit boards, gate drivers and cooling system. This may increase the volume, especially for the MDAB where a circuit board must be produced for each module.

Both converter has been simulated using simplified models. By including the generator, umbilical cable and loads in the model a more realistic model would be achieved. While a more realistic model could enhance or even deteriorate the design of the converters, the simplified models works fine for the simple converter design. The goal of this thesis is not to design the converter in detail but to discuss and propose a possible converter design for the ROV application. Therefore, the simple model simulation is regarded as good enough for this first stage of research for the fully electric ROV.

Since there is no data available for the transformer on the existing ROVs, it is not possible to compare the power electronic solution to the conventional transformer solution. However, in order to have a power density at the same level as for the MDAB the transformer needs to have an efficiency of approximate 16 kW/dm^3 to have the same power density as the power electronic solution. This is highly unlikely, as the transformers used today are low frequency transformers of either 50/60 Hz or up to 800 Hz. Reported data for a 60 Hz 25 kVA transformer with a voltage of 5/0.24 kV shows a power density of 0.11 kVA/dm^3 and 0.16 kVA/kg [50].

Based on the simulated result, the advantages, and of course disadvantages, the MDAB is recommended for further investigation. The MDAB features very high-power density with commercially available products today. There is no technological gap that has to be overcome to design a commercial MDAB. Especially interesting is the possibility to scale the converter so that each MDAB could be modularized itself in order to achieve higher output power for the different ROV sizes. While the MDAB requires further research in order to fully qualify it for the ROV application, it shows great promise for the range of fully electric work class ROVs.

7 Conclusions

The industry is researching the possibility to electrify the work class ROVs to increase reliability and lower maintenance and operation cost. The work class ROVs today can operate with both hydraulics and electricity. In order to fully electrifying them, the hydraulics will have to be substituted with electric power. The hydraulic power unit delivers power to the manipulators and tools, and for most of the ROVs, to the thrusters as well. By replacing them with their electrical powered counterparts, the hydraulic power unit can be removed.

The thesis focuses on the voltage conversion between the power supply from the support vessel and the ROV. The support vessel supplies the ROV with high voltage which needs to be stepped down to a low voltage for the ROVs components. By eliminating the hydraulic power unit, there isn't any component on the ROV which uses high voltage. Instead of using a transformer to step the voltage, a power electronic converter can be used. The power electronics enable higher power density and a higher degree of power control.

Several converter topologies have been presented and discussed. Since the ROVs need galvanic isolation between the support vessel and the ROV, isolated DC/DC converters must be used. Two of the presented converters has been further designed and simulated in an effort to come up with the most suitable topology.

The dual active bridge converter features two bridges with active switches with a transformer between. The transformer is designed with an internal energy storage inductor for the converter. The converter is designed with IGBTs as the switching devices. This limits the switching frequency and thus limiting the power density of the converter. The DAB is a simple and easy controlled converter with a well-known operation scheme.

In an effort to increase the power density, a modularized converter has been proposed. The modules consist of the same DAB as mentioned above, but with low voltage switches instead of IGBTs. The low voltage switches are able to switch with a higher switching frequency, thus leading to lower passive components and increased power density. The modularized dual active bridge is designed with both SiC devices and GaN devices to compare the volume and weight of the different configurations. The choice of switching devices has very little impact on the total converter volume and weight when it comes to low voltage discrete switching devices. In fact, the dominate part of the converter is the isolating transformer. The transformer design is not a part of the scope for this thesis, so other proposed high frequency transformer has been used as reference for the transformer power density.

When comparing the DAB and the modularized DAB, the modularized show a great reduction in volume and weight. By using low voltage switching devices, the switching frequency can be raised considerably. The MDAB design has a reduced volume of up to 69 % compared to the DAB. Due to the MDAB scalability and performance, it is recommended to further research the design to qualify it for the ROV application.

8 Further work

During this thesis, several research possibilities has been identified in order to implement a power electronic converter for the fully electric ROV. The topics will lead to different direction for the converters, but at this stage they may all be reasonable to research.

The designed DAB converter in this thesis uses IGBTs as switching devices. SiC MOSFETs are being researched as an alternative for the Si IGBTs. The MOSFETs are being developed with blocking voltages of over 10 kV. While the IGBTs low maximum switching frequency at turn-off due to the tail currents, the MOSFETs do not have these issues. These means that MOSFETs can be switch at higher speeds, which leads to a smaller and more compact MV/MP converter. These devices are still not commercialized, but test devices can be provided by the manufacturers for researchers who wants to study them for their application.

The transformer also must be design appropriately for the converters specification. The design should focus more on power density rather than achieving the highest possible efficiency. The ROV application does not focus on efficiency, but reliability and volume constraints are prioritized.

When a transformer is designed and the switching device is selected, the capacitance needs to be optimized. By properly choosing and tuning the control system it may be possible to have lower capacitance for the output voltage in order to stay within the ripple limits.

The modularized DAB should also have a proper designed transformer. Each module will have a transformer, so the transformer should be compact and small. The energy storage inductor should also be designed. As seen in [29], the inductor could be designed as an adaptive inductor to enhance the performance of the converter. A prototype module should in the end be built to further test and evaluate the performance and design.

9 References

[1] R. D. Christ and R. L. Wernli, The ROV manual, Second edition, Elsevier Ltd., 2014.

[2] Forum Energy Technologies, "Perry XLX 200Hp," [Online]. Available: http://www.f-e-t.com/products/drilling-and-subsea/subsea-technologies/rovs-work-class/triton-xls-heavy-duty-work-class-rov. [Accessed 12 November 2017].

[3] N. Vedachalam, A. Umapathy, R. Ramesh, S. M. Babu, D. Muthukumaran, A. Subramanian, G. Harikrishnan, G. A. Ramadass and M. A. Atmanand, "Ampacity Derating Analysis of Winch-Wound Power Cables: A Study Based on Deep-Water ROV Umbilical," *IEEE Journal of oceanic egnineering,* 2 April 2016.

[4] Tecnadyne, "Brushless DC Electric Thrusters," [Online]. Available: http://tecnadyne.com/thrusters/. [Accessed 14 November 2017].

[5] P. Snary, C. M. Bingham and D. A. Stone, "Influence of ROV umbilical on power quality when supplying electrical loads," Department of Electronic and Electrical Engineering, University of Sheffield, 2005.

[6] Oceaneering, "Oceaneering eNovus ROV Datasheet," [Online]. Available: https://www.oceaneering.com/datasheets/ROV-eNovus.pdf. [Accessed 13 November 2017].

[7] H. Edvardsen, "[Unpublished] Literature study of power electronic converters for work class remotely operated vehicles," Norwegian University of Science and Technology, Specializing project, 2017.

[8] A. Iversen and R. Hansen, Interviewees, *APPENDIX A, Technical ROV interview.* [Interview]. 11 April 2018.

[9] On Semiconductor, "N-Channel Power MOSFET, 1700V, 3A, 10.5Ohm, TO-3PF-3L," [Online]. Available: http://www.onsemi.com/PowerSolutions/product.do?id=WPH4003. [Accessed 2 December 2017].

[10] A. Marzoughi, A. Romero, R. Burgos and D. Boroyevich, "Comparing the state-of-the-art SiC MOSFTEs," *IEEE Power Electronics Magazine,* June 2017.

[11] N. Mohan, T. M. Undeland and W. P. Robbins, Power Electronics Converters, Application, and Design, John Wiley & Sons, Inc., 2003.

[12] J. L. Hostetler, *6.5 kV Silicon Carbide Half-Bridge Power Switch Module For Energy Storage System Application,* United Silicon Carbide inc., 2012.

[13] B. J. Baliga, Advanced Power MOSFET Concepts, Springer, 2010.

[14] A. Kadavelugu, S. Baek, S. Dutta, S. Bhattacharya, M. Das, A. Agarwal and J. Scofield, "High-frequency Design Considerations of Dual Active Bridge 1200 V SiC MOSFET DC-DC Converter," IEEE Applied Power Electronics Conference, 2011.

[15] GaN Systems, *Bottom-side cooled 650 V E-mode GaN transistor Preliminary Datasheet,* GaN Systems, 2018.

[16] J. W. Kolar, J. Biela and G. Ortiz, "Optimized Design of Medium Frequency Transformers with High Isolation Requirements," ETH Zürich.

[17] M. Mogorovic and D. Dujic, "High power MFT design optimization," École Polytechnique Fédérale de Lausanne - Power Electronics Laboratory, 2017.

[18] M. Hernes, "Pressure tolerant packaging of medium voltage converter components," Sintef Energy Research, 2015.

[19] L. Heinemann, "An Actively Cooled High Power, High Frequency Transformer with High Insulation Capability," ABB High Voltage Products, Hanau, Germany, 2002.

[20] T. Elgstrøm and L. Nordgren, "Evaluation and Design of High Frequency Transformers for On Board Charging Applications," Chalmers University of Technology, 2016.

[21] W. Shen, "Design of High-density Transformers for High-frequency High-power Converters," Virginia Polytechnic Institute and State University, 2016.

[22] D. Rothmund, G. Ortiz, T. Guillod and J. W. Kolar, "10kV SiC-Based Isolated DC-DC Converter for Medium Voltage-Connected Solid-State Transformers," ETH Zurich, 2015.

[23] B. Zhao, Q. Song, W. Liu and Y. Sun, "Overview of Dual-Active-Bridge Isolated Bidirectional DC-DC Converter for High-Frequency-Link Power-Conversion System," *IEEE Transaction on power electronics,* August 2014.

[24] S. Helland, "Evaluation of a medium-voltage high-power bidirectional dual active bridge DC/DC converter for marine application," Norwegian University of Science and Technology, Trondheim, 2017.

[25] R. L. Steigerwald, R. W. De Doncker and M. H. Kheraluwala, "A Comparison of High-Power DC-DC Soft-Switched Converter Topologies," *IEEE Transaction on industry application,* September/October 1996.

[26] F. Krismer, "Modeling and optimization of bidirectional dual active bridge DC-DC converter topologies," ETH ZURICH, 2010.

[27] M. Fazlali and M. Mobarrez, "Design, simulation and evaluation of two different topologies for the 2.4 MW 4/6 kV DC-DC fullbridge converter," Chalmers university of technology, Gõteborg, 2012.

[28] Z. Xuan, H. Shenghua and N. Guoyun, "A Three-phase Dual Active Bridge Bidirectional ZVS DC/DC Converter," *Physics Procedia 24,* 2012.

[29] H. Fan and H. Li, "High-frequency transformer isolated bidorectional DC-DC converter modules with high efficiency over wide load range for 20 kVA solid-state transformer," *IEEE Transaction on power electronics,* December 2011.

[30] G. D. Demetriades, "On Small-Signal Analysis And Control Of The Single- And The Dual-Active Bridge Topologies," Royal Institute Of Thechnology, KTH, Stockholm, 2005.

[31] B. Zhao, Q. Song and W. Liu, "Power Characterization of Isolated Bidirectional Dual-Active-Bridge DC–DC Converter With Dual-Phase-Shift Control," *IEEE Transaction on power electronics,* September 2012.

[32] H. Bai and C. Mi, "Eliminate reactive power and increase system efficiency of isolated bidirectional dual-active-bridge DC-DC converters using novel dual-phase-shift control," *IEEE Transaction on power electronics,* November 2008.

[33] F. Krismer and J. W. Kolar, "Accurate Small-Signal Model for the Digital Control of an Automotive Bidirectional Dual Active Bridge," *IEEE Transaction on power electronics,* December 2009.

[34] C. W. d. S. Kuiyuan Wu and W. G. Dunford, "Stability Analysis of Isolated Bidirectional Dual Active Full-Bridge DC–DC Converter With Triple Phase-Shift Control," *IEEE Transaction on power electronics,* April 2012.

[35] H. Fan and H. Li, "A Distributed Control of Input-Series-Output-Parallel Bidirectional DC-DC Converter Modules Applied for 20 kVA Solid State Transformer," *IEEE Transaction on power electronics,* April 2011.

[36] GaN Systems, "GaN Systems," [Online]. Available: https://gansystems.com/gan-transistors/faq/#toggle-id-39. [Accessed 05 26 2018].

[37] Infineon Technologies AG, *Datasheet IGBT FZ400R12KS4P - 1200 V - 400 A.*

[38] Infineon Technologies AG, *Datasheet IGBT FZ400R33KL2C_B5 - 1200 V - 400 A.*

[39] Powerex Inc, *Datasheet IGBT QID4515004 - 4500 V - 150 A.*

[40] Infineon Technologies AG, *Datasheet IGBT FZ250R65KE3 - 6500 V - 250 A.*

[41] STMicroelectronics, *Datasheet SiC MOSFET SCTW100N65G2AG - 650 V - 100 A.*

[42] STMicroelectronics, *Datasheet SiC MOSFET SCT20N120 - 1200 V - 20 A.*

[43] STMicroelectronics, *Datasheet SiC MOSFET SCT50N120 - 1200 V - 65 A.*

[44] GaN Systems, *Datasheet GaN Transistor GS66504B - 650 V - 15 A.*

[45] GaN Systems, *Datasheet GaN Transistor GS66508B - 650 V - 30 A.*

[46] GaN Systems, *Datasheet GaN Transistor GS66516B - 650 V - 60 A.*

[47] N. Bingham, "Designing pressure-tolerant electronic systems," March 2013. [Online]. Available: http://uutech.com/ptepaper. [Accessed 26 September 2017].

[48] Vishay BCcomponents, *Datasheet Capacitor MKP385.*

[49] B. Zahedi and L. E. Norum, "Modeling and Simulation of All-Electric Ships With Low-Voltage DC Hybrid Power Systems," IEEE Transaction on power electronics, 2013.

[50] J. W. Kolar and T. Guillod, *Medium-Frequency Transformer For Smart Grid Applications: Challenges and Opportunities,* ETH Zürich, 2016.

[51] J. W. Kolar, Writer, *Power magnetics @ high frequency.* [Performance]. ETH Zürich, 2018.

[52] Vacuumschmelze GmbH & Co, "Power transformer," October 2016. [Online]. Available: http://www.vacuumschmelze.com/fileadmin/Medienbiliothek_2010/Downloads/KB/PI-IA_5.pdf. [Accessed 20 February 2018].

Appendix A – Phone interview with Oceaneering Stavanger

Interviewer: Håvard Edvardsen
Interviewee: Arne Iversen and Rune Hansen

1. Do you have a load profile for the power consumption during operation?

   No, we don't have a load profile. However, during start up the power consumption is mainly from the losses in the system and some small electronic components. It is around 200 W. During operation the power consumption is usually around 20 % of rated power. The power is rarely at fully rated power. Still, the ROV must be designed for the fully rated power.

2. Is there galvanic isolation on the hydraulic ROVs?

   A transformer I placed on the ROV to transform the high voltage to low voltage for the equipment on board. This transformer creates the galvanic isolation. But mostly the galvanic isolation is not needed. The only requirement is that there is an isolation monitoring system connected to the ROV feeder from the support vessel.

3. What is the voltages used for the ROV?

   For the hydraulic ROV high voltage around 3 kV is used from the vessel to the ROV and HPU unit. On the ROV 110 and 24 V is used. For electric propulsion and tooling 400 VAC 60 Hz is used.

4. Are Oceaneering researching fully electric ROVs?

   No, at the moment we are not.

5. Have Oceaneering considered DC voltage supply from the vessel to the ROV?

   No, we haven't.

Appendix B – Tables

Calculated and measured values from Simulink simulation of the DAB converter

F_{sw} [kHz]	P_{out} [W]	V_{out} [V]	V_{in} [V]	L_{boost} [µH] (Calculated)	C_{out} [µF] (Calculated)	C_{out} [µF] (5% ripple)	C_{out} [µF] (10% ripple)	ΔV [V]	ΔV [%]
5	200	700	6000	493,0	202,9	520	265	69,2	9,89
10	200	700	6000	246,5	101,4	235	120	69,5	9,93
15	200	700	6000	164,3	67,6	140	71	69,7	9,96
20	200	700	6000	123,2	50,7	100	48	69,9	9,99
30	200	700	6000	82,2	33,8	55	27	69,4	9,91
40	200	700	6000	61,6	25,4	35	17	69,6	9,94
50	200	700	6000	49,3	20,3	25	12	69,7	9,96
60	200	700	6000	41,1	16,9	19	8,9	69,3	9,90
70	200	700	6000	35,2	14,5	14	6,9	69,9	9,99
80	200	700	6000	30,8	12,7	11	6	68,7	9,81
90	200	700	6000	27,4	11,3	8,5	5	68,2	9,74
100	200	700	6000	24,6	10,1	7,1	3,7	68,8	9,83
150	200	700	6000	16,4	6,8	3,7	1,75	69,1	9,87
200	200	700	6000	12,3	5,1	2,1	1,03	68,4	9,77

Calculated and measured values from Simulink simulation of the MDAB converter

F_{sw} [kHz]	P_{out} [W]	V_{out} [V]	V_{in} [V]	L_{boost} [µH] (Calculated)	C_{out} [µF] (Calculated)	C_{out} [µF] (5% ripple)	C_{out} [µF] (10% ripple)	ΔV [V]	ΔV [%]
5	200	400	4000	160,0	625,0	2500	1300	39,2	9,80
10	200	400	4000	80,0	312,5	1200	620	39,9	9,98
15	200	400	4000	53,3	208,3	800	410	39,4	9,85
20	200	400	4000	40,0	156,3	570	295	39,6	9,90
30	200	400	4000	26,7	104,2	400	190	38,7	9,68
40	200	400	4000	20,0	78,1	260	132	39,9	9,98
50	200	400	4000	16,0	62,5	200	101	39,4	9,85
60	200	400	4000	13,3	52,1	160	83	38,7	9,68
70	200	400	4000	11,4	44,6	132	67	39,2	9,80
80	200	400	4000	10,0	39,1	107	55	39,5	9,88
90	200	400	4000	8,9	34,7	95	48	38,9	9,73
100	200	400	4000	8,0	31,3	82	42	39,1	9,78
150	200	400	4000	5,3	20,8	45	24	38,5	9,63
200	200	400	4000	4,0	15,6	28	14,5	38,6	9,65

Appendix C – MATLAB script (DAB converter)

```
f_sw = 15000;
Ts = 1/f_sw;

U_ref = 700;

C_out = 71e-6;
L_boost = 165e-6;


% PI-controller %

PI_p = 1/30e6;
PI_i = 0.1/1350;

sat_upper = Ts/4;
sat_lower = 0;


% Pulse generator %

period = Ts;
pulse_width = 49;
phase_delay = Ts/2;
```

Appendix D – MATLAB script (MDAB converter)

```
f_sw = 50000;
Ts = 1/f_sw;

n = 10;
n_modules = 10;

C_out = 10.1e-6;
L_boost = 16e-6/10;

V_in = 4000;
U_ref = 400;

voltage_filter = 1e-7;


% PI-controller %

PI_p = 1/150e6;
PI_i = 0.1/350;

sat_upper = Ts/4;
sat_lower = 0;


% Transformer %

T_pn = 10e3;

T_V1 = V_in/n;
T_R1 = 0.52/n;
T_L1 = 3e-6/n;

T_V2 = 500;
T_R2 = T_R1;
T_L2 = T_L1;

T_Rm = 1.32e6;
T_Lm = 25e-3;


% Pulse generator %

period = Ts;
pulse_width = 49;
phase_delay = Ts/2;
```